

**PHYSICOCHEMICAL PROPERTIES OF VANADIUM PHOSPHORUS  
OXIDE CATALYSTS SYNTHESISED FROM DIFFERENT PREPARATION  
ROUTES**

**WONG PEI WEN**

**A project report submitted in partial fulfilment of the  
requirements for the award of Bachelor of Engineering  
(Hons.) Chemical Engineering**

**Faculty of Engineering and Science  
Universiti Tunku Abdul Rahman**

**May 2011**

## DECLARATION

I hereby declare that this project report is based on my original work except for citations and quotations which have been duly acknowledged. I also declare that it has not been previously and concurrently submitted for any other degree or award at UTAR or other institutions.

Signature : \_\_\_\_\_

Name : Wong Pei Wen

ID No. : 07UEB06571

Date : 13 May 2011

**APPROVAL FOR SUBMISSION**

I certify that this project report entitled “**PHYSICOCHEMICAL PROPERTIES OF VANADIUM PHOSPHORUS OXIDE CATALYSTS SYNTHESISED FROM DIFFERENT PREPARATION ROUTES**” was prepared by **WONG PEI WEN** has met the required standard for submission in partial fulfilment of the requirements for the award of Bachelor of Engineering (Hons.) Chemical Engineering at Universiti Tunku Abdul Rahman.

Approved by,

Signature : \_\_\_\_\_

Supervisor : Dr. Leong Loong Kong

Date : 13 May 2011

The copyright of this report belongs to the author under the terms of the copyright Act 1987 as qualified by Intellectual Property Policy of University Tunku Abdul Rahman. Due acknowledgement shall always be made of the use of any material contained in, or derived from, this report.

© 2011, Wong Pei Wen. All right reserved.

## ACKNOWLEDGEMENTS

I would like to thank everyone who had contributed to the successful completion of this project. Firstly, I would like to express my gratitude to my research supervisor, Dr. Leong Loong Kong for his invaluable advice, guidance and his enormous patience throughout the development of the research.

In addition, I would also like to express my gratitude to the seniors who have been helping and guiding me from the beginning of synthesis till the end of the thesis writing. I'll also never forget to thank my coursemates and teammates who had helped and given me encouragement throughout the project.

Finally, never forget my parents who have been the ones supporting me morally and financially throughout my degree in university.

**PHYSICOCHEMICAL PROPERTIES OF VANADIUM PHOSPHORUS  
OXIDE CATALYSTS SYNTHESISED FROM DIFFERENT PREPARATION  
ROUTES**

**ABSTRACT**

Four different methods were used to prepare the V-P-O catalysts. VPA, by digesting  $V_2O_5$  in concentrated HCl prior to the addition of  $H_3PO_4$ . VPO, by reacting  $V_2O_5$  with  $H_3PO_4$  in a mixture of isobutanol and benzyl alcohol. VPD, by reacting  $VOPO_4 \cdot 2H_2O$  with isobutanol. VPS, by reacting  $VOPO_4 \cdot 2H_2O$  with 1-butanol. Precursor from sesquihydrate route denoted as VPSP showed the characteristic reflections of vanadium phosphate sesquihydrate,  $VOHPO_4 \cdot 1.5H_2O$  whereas the other three precursors showed the phase of vanadium phosphate hemihydrates,  $VOHPO_4 \cdot 0.5H_2O$ . All the precursors were successfully transformed to the catalyst vanadyl pyrophosphate after undergoing calcinations in a flow of 1.1% oxygen/nitrogen at 733 K for 24 hours. Although VPA24 showed the highest crystallinity, its surface area was very small ( $6.232 \text{ m}^2 \text{ g}^{-1}$ ) which was due to the large crystallite size. VPO24 on the other hand gave the largest surface area of  $26.638 \text{ m}^2 \text{ g}^{-1}$ . The vanadium species of the V-P-O catalysts were mostly comprised of  $V^{4+}$  species with little of presence  $V^{5+}$  species. The P/V atomic ratio obtained from all the catalysts were within the optimal range which was from 1.01 to 1.30. Scanning electron microscopy showed the catalysts produced from organic and sesquihydrate route consist of plate-like crystals which were agglomerated into rosette-shape clusters. More splits were found in VPO24 catalyst that had caused the surface area to be higher compared to the other catalysts. VPA24 did not possess rosette shape but appeared to be large and square platelets which caused its surface area to be comparably lower. VPD24 on the other hand also showed no rosette shape clusters but consist of small and round platelets that are closely packed together.

## TABLE OF CONTENTS

<b>DECLARATION</b>	<b>ii</b>
<b>APPROVAL FOR SUBMISSION</b>	<b>iii</b>
<b>ACKNOWLEDGEMENTS</b>	<b>v</b>
<b>ABSTRACT</b>	<b>vi</b>
<b>TABLE OF CONTENTS</b>	<b>vii</b>
<b>LIST OF TABLES</b>	<b>x</b>
<b>LIST OF FIGURES</b>	<b>xi</b>
<b>LIST OF SYMBOLS / ABBREVIATIONS</b>	<b>xiii</b>
<b>LIST OF APPENDICES</b>	<b>xiv</b>

### CHAPTER

<b>1</b>	<b>INTRODUCTION</b>	<b>1</b>
	1.1 Catalysis	1
	1.2 Catalysts	1
	1.3 Types of Catalysts	2
	1.3.1 Homogeneous Catalysts	2
	1.3.2 Heterogeneous Catalysts	3
	1.3.3 Biocatalysts	5
	1.4 Energy Profile of Reaction with Catalysts	6
	1.5 Essential Properties of Good Catalysts	7
	1.6 Importance and Uses of Catalysts	8
	1.7 Problem Statements	8
	1.8 Objectives of Research	9

<b>2</b>	<b>LITERATURE REVIEW</b>	<b>10</b>
2.1	Vanadium Pyrophosphate Catalyst (VO) <sub>2</sub> P <sub>2</sub> O <sub>7</sub>	10
2.2	Preparation of Vanadium Phosphorus Oxide Catalyst	11
2.2.1	Aqueous Method	12
2.2.2	Organic Method	12
2.2.3	Dihydrate Precursor Route	13
2.2.4	Sesquihydrate Precursor Route	13
2.3	Parameters	14
2.3.1	Calcinations Temperature	14
2.3.2	Calcinations Duration	15
2.3.3	Calcinations Environment	15
2.3.4	Doped System	16
2.3.5	P/V Atomic Ratio	17
2.4	Maleic Anhydride	18
<b>3</b>	<b>METHODOLOGY AND CHARACTERISATION TECHNIQUES</b>	<b>20</b>
3.1	Materials	20
3.2	Methodology	21
3.2.1	Catalysts Preparation via Aqueous Route	21
3.2.2	Catalysts Preparation via Organic Route	22
3.2.3	Catalysts Preparation via Dihydrate Route	22
3.2.4	Catalysts Preparation via Sesquihydrate Route	22
3.3	Characterisation Techniques and Instrumentation	25
3.3.1	X-Ray Diffraction (XRD) Analysis	25
3.3.2	BET Multi Point Surface Area Measurement	27
3.3.3	Redox Titration	29
3.3.4	Scanning Electron Microscopy (SEM)	30
3.3.5	Energy Dispersive X-Ray (EDX)	32
3.3.6	Inductively Coupled Plasma Optical Emission Spectrometry (ICP-OES)	33

<b>4</b>	<b>RESULTS AND DISCUSSION</b>	<b>35</b>
4.1	Introduction	35
4.2	X-Ray Diffraction Analysis	36
4.3	BET Multipoint Surface Area Measurements	39
4.4	Chemical Analysis	40
4.4.1	Chemical Compositions	40
4.4.2	Oxidation State of Vanadium	41
4.5	Scanning Electron Microscopy	43
<b>5</b>	<b>CONCLUSIONS AND RECOMMENDATIONS</b>	<b>46</b>
5.1	Conclusions	46
5.2	Recommendations	47
	<b>REFERENCES</b>	<b>48</b>
	<b>APPENDICES</b>	<b>52</b>

**LIST OF TABLES**

<b>TABLE</b>	<b>TITLE</b>	<b>PAGE</b>
1.1	Steps in a heterogeneous catalytic reaction	4
4.1	XRD data of V-P-O catalysts.	39
4.2	BET surface area analysis of V-P-O catalyts	40
4.3	Chemical compositions and average oxidation numbers	41

## LIST OF FIGURES

<b>FIGURE</b>	<b>TITLE</b>	<b>PAGE</b>
1.1:	Reaction cycle of biocatalysis	5
1.2:	Energy profile of catalysed and uncatalysed reactions	6
2.1:	Idealized structure of vanadyl pyrophosphate	11
2.2:	Occurrence of sintering effect	14
2.3:	Reaction mechanism from <i>n</i> -butane to maleic anhydride	19
3.1:	Transformation from precursor to catalyst	23
3.3:	Flow diagram of sesquihydrate preparation route	24
3.3:	Two X-ray beams directed to parallel crystallographic planes	26
3.4:	Shimadzu diffractometer model XRD-6000	27
3.5:	Thermo Finnigan Sorptomatic 1990	28
3.6:	Scanning electron microscopy	31
3.7:	Hitachi S4300N	32
3.8:	Shells that may present in an atom	33
3.9:	Perkin-Elmer Emission Spectrometer Model Plasma	34
4.1:	XRD patters of precursors VPAP, VPOP, VPDP, and VPSP	36
4.2:	XRD patterns of VPA24, VPO24, VPD24, and VPS24 catalysts	38

4.3:	SEM micrographs of VPA24	43
4.4:	SEM micrographs of VPO24	44
4.5:	SEM micrographs of VPD24	44
4.6:	SEM micrographs of VPS24	45

**LIST OF SYMBOLS / ABBREVIATIONS**

$\alpha$	alpha
$\beta$	beta
$\delta$	delta
$\gamma$	gamma
$\omega$	omega
<i>o</i>	ortho
$\theta$	theta
BET	Brunauer Emmett Teller
XRD	X-Ray Diffraction
SEM	Scanning Electron Microscopy
EDX	Energy Dispersive X-Ray
ICP-OES	Inductively Coupled Plasma - Optical Emission Spectrometry
FWHM	Full-Width at Half Maximum
JCDPS	Joint Committee on Powder Diffraction Standards
MA	Maleic Anhydride
VPO	Vanadium Phosphorus Oxide
P/V	Phosphorus/Vanadium

**LIST OF APPENDICES**

<b>APPENDIX</b>	<b>TITLE</b>	<b>PAGE</b>
A	Volume of Isobutanol Used	52
B	Volume of Distilled Water Used	54
C	Crystallite Size Measurement (XRD Analysis)	55
D	Preparation of Diphenylamine, Ph <sub>2</sub> NH Indicator	56
E	Preparation of 2 M Sulphuric Acid, H <sub>2</sub> SO <sub>4</sub> Solution	57
F	Preparation of 0.1 M Sulphuric Acid, H <sub>2</sub> SO <sub>4</sub> Solution	58
G	Preparation of 0.01 N Potassium Permanganate, KMnO <sub>4</sub> (Redox Titration)	59
H	Preparation of 0.01 N Ammonium Iron(II) Sulphate, (NH <sub>4</sub> ) <sub>2</sub> Fe(SO <sub>4</sub> ) <sub>2</sub> · 6H <sub>2</sub> O (Redox Titration)	60
I	Oxidation State of Vanadium (Redox Titration)	61

## CHAPTER 1

### INTRODUCTION

#### 1.1 Catalysis

Catalysis is the phenomenon at which a substance, known as catalyst is used to alter the rate of a chemical reaction. This technology is widely used in all chemical industries by both scientists and engineers. A catalyst induces changes in the reaction pathway that will increase the reaction rate. More specifically, catalysts could change the attainment rate of chemical equilibrium without themselves being changed or consumed in the process [Armor, 2008]. According to Mittasch (1999), “chemistry without catalysis would be a sword without handle... or a bell without sound”.

Though the presence of catalysts could speed up a given chemical reaction, a catalyst may slow down a reaction too, which in this case, is termed negative catalyst (inhibitor). On the other hand, catalyst that promotes the reaction to be faster is termed positive catalyst.

#### 1.2 Catalysts

In terms of chemistry, catalyst is a substance that is added in a small amount to accelerate a chemical reaction. Compared to uncatalysed reactions, catalysts provide a different molecular path (“mechanism”) for the reaction [Fogler, 2008]. Usually, this different mechanism will have a lower activation energy, by which the reactants

could easily react to form products. It is said that a catalyst offers an alternative, energetically favourable mechanism to the non-catalytic reaction, thus enabling processes to be carried out under industrially feasible conditions of pressure and temperature [Chorkendoff and Niemantsverdriet, 2003].

A catalyst only affects the rate of a chemical reaction, but it would not affect the equilibrium. The standard entropy and enthalpy changes are equal for both the catalysed and uncatalysed reaction. Hence, if a reaction is thermodynamically unfeasible, the use of catalyst would not change this situation. A catalyst changes only the kinetics, but not the thermodynamics [Chorkendoff and Niemantsverdriet, 2003]. In addition, for a given reaction, a catalyst will increase the forward and reverse reaction rates to the same extent.

In a catalytic reaction, a catalyst alters the rate of a chemical reaction leaving itself unaltered. It forms bonds with reactants which then react to form products. The products will detach from the catalyst without any chemical change that it is available for the next reaction. However, in reality, as the catalysts are used, they can be slowly inhibited, deactivated or destroyed by secondary processes [Fogler, 2008].

### **1.3 Types of Catalysts**

#### **1.3.1 Homogeneous Catalysts**

Homogeneous catalysis concerns processes in which a catalyst is in solution with at least one of the reactants [Fogler, 2008]. In normal operations, these processes will take place either in gas or liquid phase where only one phase will occur. A typical example of homogeneous catalysis in liquid phase is the Oxo process for manufacturing normal isobutylaldehyde. Reactants consist of propylene, carbon monoxide, and hydrogen react in the presence of liquid-phase cobalt complex. Another example of homogeneous catalysis is the ozone decomposition which is

accelerated in the presence of Cl atom. Both reactant and catalyst are in the same gaseous phase.

The main advantage of using homogeneous catalyst is its specificity to a desired product. This is due to its specific structure whereby it contains only one type of active site. According to Hertly (1985), homogeneous catalysts are more reproducible compared to heterogeneous catalysts because homogeneous catalysts have a definite stoichiometry and structure.

Although homogeneous catalysts have very specific active sites, their use in industrial applications often give troubles and difficulties in the separation of product from catalyst at the end of reaction. High purity of product can only be obtained through large separation processes such as distillation or ion-exchange. Employment of these processes could greatly increase the overall cost of production. Moreover, it is hard to achieve a high end quality product due to the presence of small catalyst that may contaminate the product especially in food industry [Ramaswamy, 2002]. This is strictly unacceptable as some of catalyst components could cause death among human.

### **1.3.2 Heterogeneous Catalysts**

Heterogeneous catalysis involves processes more than one phase. In normal operations, the catalyst is a solid and the reactants and products are in liquid or gaseous form [Fogler, 2008]. For example, in the production of benzene, cyclohexane is dehydrogenated using platinum-on-alumina as the catalyst.

Using a heterogeneous catalyst, the reaction occurs at or very near the fluid-solid interface [Fogler, 2008]. In order for a reaction to occur, reactants have to attach themselves to the catalyst solid surface. There are two different processes at which adsorption can take place: physical adsorption and chemisorption. For physical adsorption, weak van der Waals forces exist between the gas molecules and

the solid surface. On the other hand, the chemisorption process will affect the rate of chemical reaction whereby the adsorbed reactant molecules are held to the surface by valence forces [Somorjai, 1994].

Generally in heterogeneous catalytic reactions, there are mainly 7 steps involved as shown in Table 1.1:

**Table 1.1: Steps in a heterogeneous catalytic reaction**

---

1. Mass transfer of reactants from the bulk fluid to the external surface of the catalyst pellet
2. Diffusion of reactant from the pore mouth through catalyst pores to the internal catalytic surface
3. Adsorption of reactant on the catalyst surface
4. Reaction to form product on the surface
5. Desorption of the products from the surface
6. Diffusion of the products from the interior through the pore mouth to the external surface
7. Mass transfer of the products from the external surface to the bulk fluid

---

[Fogler, 2008]

One of the steps above could be the rate determining step and it will be the slowest among all. For most cases, the surface reaction is the rate limiting step. Furthermore, there are many models that describe the surface reaction which include single site, dual site, Langmuir-Hinshelwood kinetics as well as Eley-Rideal mechanism [Hinshelwood, 1940].

In comparison to homogeneous catalysts, heterogeneous catalysts are easier to separate from the end product by using simple method such as coarse filtration. Since some catalysts consist of expensive metals such as rhodium and platinum, they can be reused and regenerate lowering the overall production cost. In addition, Noritaka and Makota (1997) said that the thermal stability of heterogeneous catalysts are always much higher than that of homogeneous catalysts. Hence, for operations in high temperature, heterogeneous catalytic reactions are always more favourable.

However, the disadvantage of using heterogeneous catalysts is that they are not easy to reproduce as structures of the surface of heterogeneous catalysts are strongly dependent on the method of preparation and their history subsequent to preparation [Hertley, 1985].

### 1.3.3 Biocatalysts

Biocatalysts which are also known as enzymes are considered as large protein molecules. The enzyme has very shape-specific active site that can be fitted with substrate having a specific structure. Hence, enzymes are highly specific and very efficient catalysts. Reactants or substrates that can form optimum configuration with the enzyme will form temporary bonds at the active site. This allows them to react and form products. Products usually do not have shapes or structures that fit the active site, hence they are released to the bulk fluid [Johnson 2007]. An example of biocatalysis reaction is the decomposition of hydrogen peroxide into water and oxygen that is catalysed by enzyme catalase [Chorkendoff and Niemantsverdriet, 2003].

The following Figure 1.1 shows the cycle of a biocatalysis reaction.

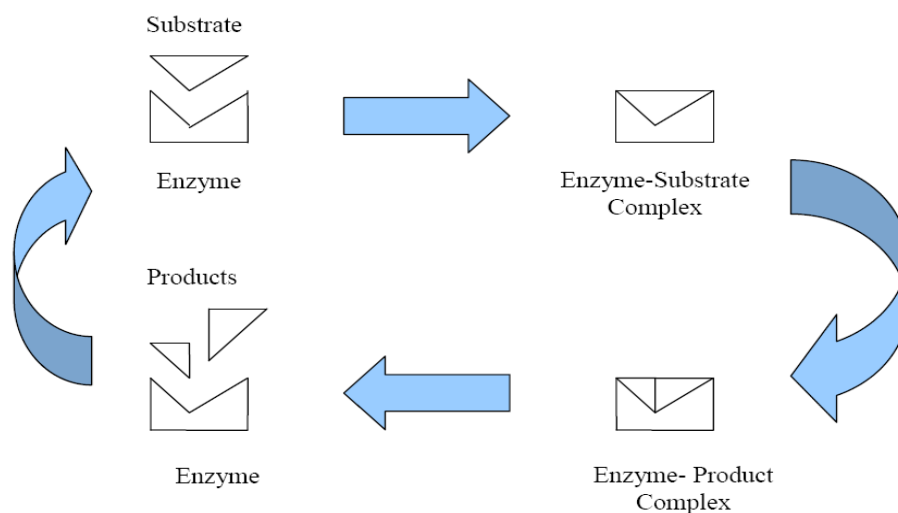


**Figure 1.1: Reaction cycle of biocatalysis**

## 1.4 Energy Profile of Reaction with Catalysts

The primary application of a catalyst is to increase the rate of chemical reaction by providing a favourable mechanism, or in other terms, by lowering the activation energy [Ramaswamy, 2002].

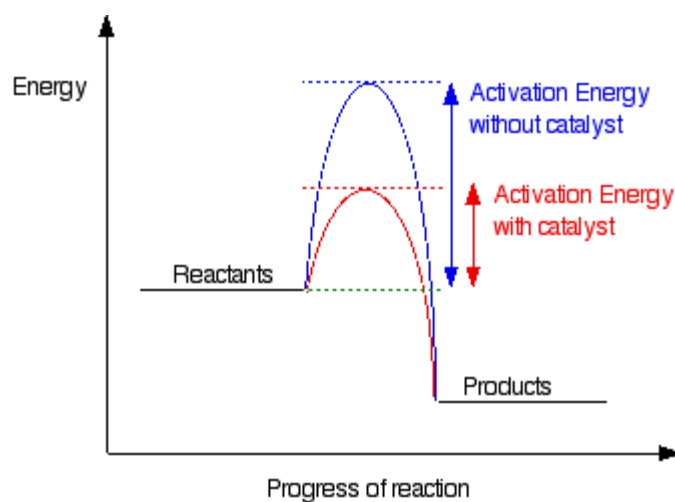


**Figure 1.2: Energy profile of catalysed and uncatalysed reactions**

[Arrhenius Equation, 1889]

Arrhenius (1889) suggested that the specific reaction rate,  $k_A$  is dependent on temperature and given by the equation

$$k_A(T) = Ae^{-E/RT} \quad (1.1)$$

where

$A$  = preexponential factor or frequency factor

$E$  = activation energy

$R$  = gas constant

$T$  = absolute temperature

The activation energy is a barrier to energy transfer (from kinetic energy to potential energy) between reactant molecules that must be overcome so that reaction occurs. From Figure 1.2, the catalysed reaction has a lower energy barrier compared

to the uncatalysed reaction. According to G.C. Bond (1987), in the presence of catalyst, the complex or the transition state formed between catalyst and reactants is immobilized. Hence, due to the loss of translational freedom, the activation energy for a catalytic reaction is usually less than that of non-catalytic reaction.

The lower activation energy allows more reactant molecules to have sufficient energy for collisions to take place. Thus, the conversion rate is higher for catalysed reaction [Fogler, 2008].

### **1.5 Essential Properties of Good Catalysts**

The key characteristics of a successful catalyst depend on its catalytic activity, selectivity, life span, possibility to regenerate and thermal stability. Parameter that is used to quantify a catalyst is the *turnover frequency* (TOF) [Fogler, 2008]. This parameter is defined as the number of reactant molecules converted per molecule of catalyst [Sharp, 2003]. Higher activity will give higher conversion rate so that the reactants are consumed effectively and wastage is minimized.

However, catalyst with high activity is not sufficient. Another important criteria is its selectivity. It is a measure of the percentage of reactants that are converted into desired products [Somorjai, 2008]. In almost any chemical reaction, there will be unavoidable side reactions to form useless by-products. For a catalytic reaction with low selectivity, many by-products are formed and the cost of separating the products will be prohibitive.

The life-span of a catalyst refers to the time which the catalyst could remain its activity and selectivity. It is important the life-span of the catalyst is known such that an engineer could plan for the production run times as well as the times for catalysts regeneration or replacement [Bond, 1987].

The catalysts' ability to be regenerated as many times would greatly benefit the industrial processes in terms of cost. Types of catalysts that are easily regenerated include metal and metal oxides [Bond, 1987]. Furthermore, the catalyst's thermal stability plays an important role in industrial applications especially those operating at high temperatures. High temperature would lead to sintering, structural change as well as volatilisation in the reaction environment [Cherkendoff and Niemantsverdriest, 2003].

## **1.6 Importance and Uses of Catalysts**

Catalysis technology are widely employed in industry whereby it is estimated around 85-90% of the products of chemical industry are made in catalytic processes. Catalysts are especially important in bulk (petroleum) and fine chemicals (pharmaceutical) and in food industry as well. Together, they account for more than 10 trillion dollars of the gross national product (GNP) [Ertl and Freund, 1999]. As described earlier, in most processes, only small amounts of catalysts are added in. Hence, catalysis costs are much less compared to the sales revenue from the products which they create.

## **1.7 Problem Statements**

This final year project was to be carried out in the focus of synthesising and characterising vanadium phosphorus oxide (V-P-O) catalysts. V-P-O catalysts are still regarded as the most effective catalyst in the production of maleic anhydride, however their low selectivity remains a serious issue.

Among all the factors that affect the performance of the catalyst, it was proposed from previous studies that the microstructure of the catalyst had a critical effect on the selectivity.

Hence, by controlling the microstructure or morphology of the catalyst, one would be able to increase the catalytic activity as well as the selectivity. A catalyst morphology can be readily controlled at the precursor stage. Many efforts had been done in order to improve the method on the preparation of the precursor.

In relation to all of the above reasons, this project was focusing on the effect of precursor preparation routes on the catalytic performance. There were four different routes, namely organic method, aqueous method, dihydrate precursor method and sesquihydrate precursor method.

## **1.8 Objectives of Research**

The objectives of this project were to :

1. To synthesise the precursors using various methods, organic, aqueous, dihydrate precursor and sesquihydrate precursor routes.
2. To synthesise the Vanadium Phosphorus Oxide (V-P-O) catalysts from the corresponding precursors.
3. To study the physical and chemical properties of the catalysts.

## CHAPTER 2

### LITERATURE REVIEW

#### 2.1 Vanadium Pyrophosphate Catalyst $(VO)_2P_2O_7$

Since 1960s, vanadium phosphorus oxide (V-P-O) catalyst had been effectively used in the selective oxidation of *n*-butane to maleic anhydride. Cavani and Trifiro (1994) reported that vanadyl pyrophosphate  $(VO)_2P_2O_7$ , generally considered as the active and selective phase in this selective oxidation of *n*-butane. According to Duvauchelle and Bordes (1998), they found out that the state of vanadyl pyrophosphate actually ranges from amorphous to crystallized depending on several factors. Some authors state that the vanadium pyrophosphate is the only catalytically active phase (Thompson, 1993 and Holmes *et al.*, 2001). In contrast, there are others who believe that the active sites in VPO catalysts are a combination of vanadyl pyrophosphate with patches of  $VOPO_4$  polymorphs (Hutchings *et al.*, 1994 and Coulston *et al.*, 1997).

Vanadyl pyrophosphate catalyst is generally prepared from its precursor, represented as  $VOHPO_4 \cdot 0.5H_2O$  and it is activated under the flow of *n*-butane/air at about 400 °C. The resulted catalyst is a complex mixture of many phases such as,  $\alpha$ -,  $\beta$ -,  $\gamma$ - $VOPO_4$ ,  $VOHPO_4 \cdot 4H_2O$ ,  $VOHPO_4 \cdot 0.5H_2O$ ,  $VO(PO_3)_2$  and  $\beta$ -,  $\gamma$ - $(VO)_2P_2O_7$  [Centi *et al.*, 1988 and Borders, 1987]. Although vanadyl pyrophosphate which is the  $V^{4+}$  phase has been known to be primarily active site, however a little presence or residual  $V^{5+}$  was observed to favor the *n*-butane transformation to maleic anhydride [Forissier *et al.*, 1994]. But the optimal ratio of  $V^{5+}/V^{4+}$  associated to best catalytic performance is still not known.

Gulians *et al.* (1993) reported that the best catalysts contained only vanadyl pyrophosphate phase with well ordered stacking of the (1 0 0) plane. Figure 2.2 shows such an idealized structure of vanadyl pyrophosphate.

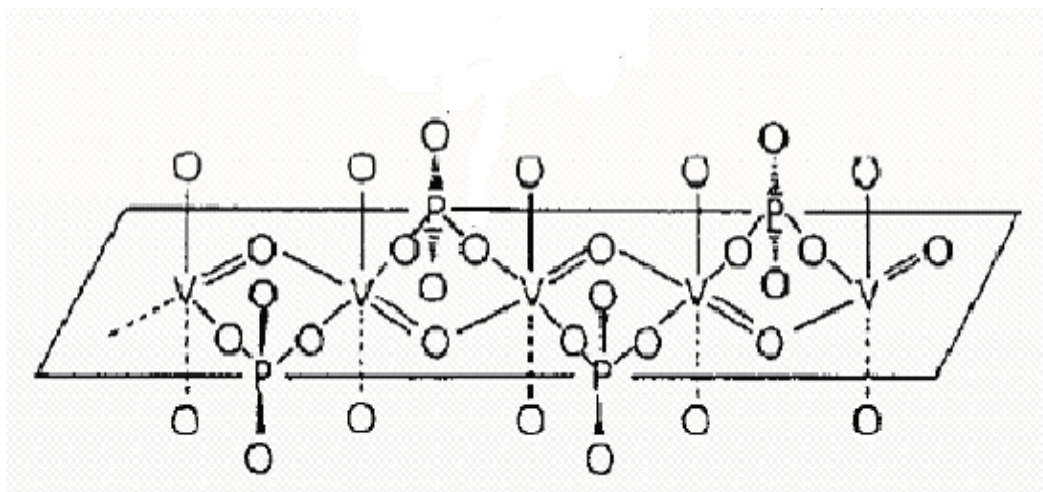


**Figure 2.1: Idealized structure of vanadyl pyrophosphate**

## 2.2 Preparation of Vanadium Phosphorus Oxide Catalyst

The catalytic performance of vanadium phosphorus oxide (V-P-O) catalyst depends on the method that it is prepared. Quite a number of preparation methods have been introduced or proposed, it was found that by employing different preparation methods, it could control the morphology of the precursor as well as the characteristics of its catalyst.

In general, vanadium pentoxide ( $V_2O_5$ ) is used as the source of vanadium while phosphoric acid ( $H_3PO_4$ ) is used as the source of phosphorus. Though different crystallites sizes and structures are obtained from different preparation methods, the nature of active sites are not affected by the preparation methods [Shima and Hatano, 1997].

There are four ways to synthesize the precursor  $VOHPO_4 \cdot 0.5H_2O$ , mainly the aqueous, organic, dihydrate precursor route and sesquihydrate precursor route.

### 2.2.1 Aqueous Method

Aqueous method is the earliest method of preparation that was done by hydrochloric acid digestion of a vanadium source prior to phosphorus source addition. The use of such mineral agents (HCl and  $N_2H_4$ ) often poses engineering difficulty, as it is corrosive to reactors and pipes.

Catalysts produced from aqueous method, although they are more crystalline [Cavani and Trifiro, 1976], but they have very low specific surface area [Hutchings, 2004]. Since catalytic activity is directly related to surface area, this preparation method is not advisable and the catalysts produced exhibit poor performance for *n*-butane selective oxidation.

### 2.2.2 Organic Method

To overcome the major disadvantage of the aqueous method, a better method is developed replacing both acid and water needed in aqueous method by organic solvents. This method is termed organic method and it is still the commercially used method in most industrial processes. Two common organic solvents are benzyl alcohol, isobutanol or a mixture of them. The precursor generated from this method is the vanadium hydrogen phosphate hemihydrates,  $VOHPO_4 \cdot 0.5H_2O$  and could be topotactically transformed to the active vanadyl pyrophosphate,  $(VO)_2P_2O_7$  catalysts after activation under reaction conditions [Johnson *et al.*, 1984]. Cavani and Trifiro (1994) reported that catalysts prepared from organic method possess larger surface area and higher density of active sites. On the other hand, the percentage crystallinity is lower for these catalysts. Since catalytic activity is proportional to the surface area and active sites, the performance is greatly enhanced for catalysts prepared from organic route.

### 2.2.3 Dihydrate Precursor Route

Dihydrate precursor route is based on alcohol reduction of  $\text{VOPO}_4 \cdot 2\text{H}_2\text{O}$ . This route is a two stage method at which in the first stage,  $\text{V}_2\text{O}_5$  reacts with  $\text{H}_3\text{PO}_4$  in water to form  $\text{V}^{5+}$  phase of  $\text{VOPO}_4 \cdot 2\text{H}_2\text{O}$ . The dihydrate is then reduced by alcohol to form  $\text{VOHPO}_4 \cdot 0.5\text{H}_2\text{O}$ . Brutovsky *et al.* (1993) claimed that precursor prepared in this way could lead to the identification of a high area preparation method of the catalyst. In addition, dihydrate precursor route can provide vanadyl pyrophosphate a better morphology that expose the preferentially (1 0 0) active plane for the selectivity towards maleic anhydride [Hutchings *et al.*, 1997]. In the same study, it was found that the precursor prepared in dihydrate method opens a new route to the synthesis of  $\text{VO}(\text{H}_2\text{PO}_4)_2$  which has the potential to be the ultra-selective catalysts in the production of maleic anhydride.

### 2.2.4 Sesquihydrate Precursor Route

Sesquihydrate precursor route is a recent alternative route from the dihydrate method [Ishimura *et al.*, 2000]. Reduction of  $\text{VOPO}_4 \cdot 2\text{H}_2\text{O}$  using 1-butanol will give  $\text{VOHPO}_4 \cdot 1.5\text{H}_2\text{O}$  which is the sesquihydrate precursor. Once the precursor is calcined under reaction conditions at 753 K, the resulted catalyst has high specific activity and selectivity towards maleic anhydride.

Due to its layered structure, the sesquihydrate precursor can be intercalated with dopants to improve its catalytic performance. For example, the sesquihydrate is doped with cobaltous acetate and had shown increase in activity, but both selectivity to maleic anhydride and surface area decreased with increasing cobalt contents [Ishimura *et al.*, 2000].

## 2.3 Parameters

Apart from the different precursor routes, there are also other parameters that could affect the morphology of the vanadium phosphorus oxide (V-P-O) catalyst and thus, affecting its catalytic performance in the synthesis of maleic anhydride.

This includes:

- Calcinations temperature
- Calcinations duration
- Calcinations environment
- Doped system
- P/V atomic ratio

### 2.3.1 Calcinations Temperature

The optimum calcinations temperature of a precursor is in the range between 380 °C to 460 °C [Taufiq-Yap *et al.*, 2001]. Catalyst prepared at a calcination temperature which is too low may not be able to form the required active phase of vanadyl pyrophosphate. However, too high calcination temperature might as well cause sintering effect to occur. Sintering effect is the phenomenon at which small sizes of crystallites aggregate together to form large particles. This is illustrated in the Figure 2.2:

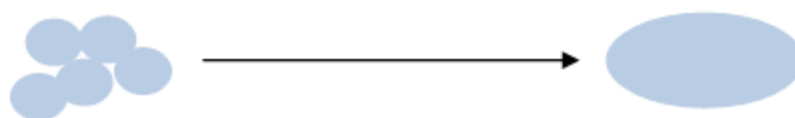


**Figure 2.2: Occurrence of sintering effect**

According to Abon and Volta (1997), the crystallinity of the vanadyl pyrophosphate phase was found to be increased with increasing calcinations

temperature. Apart from that, the crystallites sizes of the VPO catalyst increase with the calcinations temperature [Perex *et al.*, 1997].

The catalytic selectivity towards the desired product is dependent on the availability of acid sites. In the calcinations under nitrogen atmosphere, the acid sites are provided by the adsorption of ammonia on the V-P-O catalyst. Nevertheless, the adsorption diminishes by effect of calcinations temperature due to the loss of functional groups of vanadyl pyrophosphate phase [Ebner and Thompson, 1993].

### **2.3.2 Calcinations Duration**

Catalyst that is prepared from calcination duration less than 1000 hour is termed the non-equilibrated catalyst. On the hand, if the catalyst is calcined more than 1000 hour, this will yield the equilibrated catalyst. The equilibrated catalysts are generally more stable under reaction conditions [Cavani and Trifiro, 1994].

From Taufiq-Yap *et al.* (2001), it was observed that the crystalline phase of vanadyl pyrophosphate increases with activation time. In addition, catalysts with longer calcination duration would have an increase in their surface area due to the increase in the number of platelets that formed the rosette structure. Longer activation time also shows a more prominent and clearer shape of the rosette agglomerates compared to those catalysts prepared under shorter calcination duration. Hence, it can be concluded that the longer duration of pretreatment under butane/air greatly enhance the activity and selectivity of the catalyst.

### **2.3.3 Calcinations Environment**

Basically, there are two main types of environments that a catalyst can be calcined. One is the conventional method used in industrial applications which is under the

flow of n-butane/air. However, catalyst may also be activated under an inert atmosphere, such as nitrogen gas. The choice of the catalyst pretreatment environment could greatly affect the catalytic performance. Hodnett *et al.* (1984) and Pyatnitskaya *et al.* (1977) claimed that calcinations under butane/air mixture give the best results. However, the choice of pretreatment gases is much dependent on the catalysts composition.

From a study conducted by Cheng and Wang (1997), the crystalline phase of vanadyl pyrophosphate ( $V^{4+}$ ) was found to be higher under inert atmosphere. The selectivity and yield of the desired product increased with the oxidising strength of calcinations environment. High selectivity is attributed to the presence of  $V^{5+}$  phase. However, up to a certain oxygen concentration, the selectivity is drastically reduced. This is because, at very high concentration of oxygen, the V-P-O catalyst may be over-oxidised and decrease the dispersion of  $V^{5+}$  species causing the formation of crystalline  $V^{5+}$  instead. Hence, the catalyst surface is reduced as well as the conversion of n-butane. Apart from the vanadium oxidation states, different calcinations environments would also affect the morphology of the calcined catalyst. The size of the platelet face decreases with the increasing oxidising strength of the calcine gaseous.

#### **2.3.4 Doped System**

The addition of dopant is actually the introduction of metal cations to the vanadium phosphorus oxide (V-P-O) catalyst in order to improve the activity and selectivity. A variety of cations or promoters may be added to V-P-O catalyst via different techniques such as reflux, dry impregnation and wet impregnation. Normally, these promoters are added in small amount, less than 10%. In addition, the promotional effect of the dopant occurs only in a narrow range of dopant concentration. According to Bartholomew and Farrauto (2006), the strength of adsorption of reactants and their amount increases with the presence of promoters.

The promoter cation induces structural defects on the catalyst at which the promoter acts as a phosphorus scavenger ensuring that the inactive low surface area phases such as  $\text{VO}(\text{H}_2\text{PO}_4)_2$  are not formed [Hutchings, 1991 and Bartley *et al.*, 2000]. Bartley and his co-workers (2000) also suggested that the excess phosphorus is typically present in these promoted catalysts as the phosphate of the added cation. In addition, the presence of a promoter cation can act as an electronic promoter and replaces the  $\text{V}^{4+}$  in the catalyst. By this way, the ratio of  $\text{V}^{4+}/\text{V}^{5+}$  is significantly reduced and hence, the catalytic performance is improved.

Normally, the promoters added have basic nature that they can easily donate electrons to the framework of vanadyl phosphate. The incorporation of such alkali or alkaline-earth metal ions would donate electrons to the V-P-O lattice with P/V ratios of 1.07 and 1.20 giving the rise of negative charge on the lattice oxygen atoms. This was determined by Zazhigalov *et al.* (1995) and was found that the conversion of *n*-butane is enhanced.

In another study, Taufiq-Yap and co-workers (1995) reported that the addition of cobalt and chromium could give rise to the amount of lattice oxygen associated with  $\text{V}^{4+}$ . Since O- $\text{V}^{4+}$  is the centre of *n*-butane activation [Herrmann *et al.*, 1997], higher yield of maleic anhydride can be produced.

The addition of dopant such as iridium into the catalysts could significantly change their oxidising ability. Catalysts that are promoted are generally more susceptible to oxidation. On contrary, unpromoted catalysts have high resistance to the oxidations during calcinations [Cheng and Wang, 1997].

### 2.3.5 P/V Atomic Ratio

It has been found that the P/V atomic ratio plays an important role in the reaction over vanadium phosphorus oxide (V-P-O) catalyst. This ratio is determined to be within 0.90-1.20 to have an optimal catalyst performance [Horowitz *et al.*, 1998].

Hence, a little excess of phosphorus from the stoichiometric would greatly enhance the catalytic activity and selectivity. In year 1998, Centi *et al.* claimed that the best catalytic performance was attributed to the catalyst with P/V ratio of 1.1.

According to Hodnett *et al.* (1983), slight excess of phosphorus delays the oxidation of the  $V^{4+}$  to  $V^{5+}$ , hence, sustaining the active phase of vanadyl pyrophosphate. At high P/V ratio, it favoured the formation of  $V^{4+}$  while low P/V ratio favoured the formation of  $V^{5+}$ . Previous studies had demonstrated that vanadyl pyrophosphate alone is not the active phase for selective oxidation of *n*-butane to maleic anhydride, a suitable  $V^{4+}/V^{5+}$  balance is required for the best performance of this material [Ait-Lachgar *et al.*, 1997]. Therefore, a suitable P/V ratio of around 1.1 would results in optimum activity and selectivity.

## 2.4 Maleic Anhydride

Maleic anhydride which is also known as cis-butanedioic anhydride has a cyclic structure with two carboxylic acid groups located next to each other in the cis- form. Maleic anhydride is a highly reactive compound due to its structure. Therefore, they can be employed in many types of reactions such as alkylation, esterification, isomerisation, polymerization and etc [Shina and Hatano, 1997].

One of its main application is the in the production of polyester resins. Polyester resins are important in the making of fibreglass composites for boats, cars and other consumer products. Apart from that, maleic anhydride has been extensively used in the production of lube oil, copolymers and its current potential in producing pesticides [Matar and Hatch, 1994].

According to Science Stuff (2002), it was estimated that the production of maleic anhydride would rise at an average annual rate of 3.1 % in the United States and 7-8 % in Asia.

Maleic anhydride is commercially produced from the partial oxidation of benzene in air. However, recently, the oxidation of butane has become more common. This is because the butane gases are comparably less expensive, less toxic and they can be easily available. Benzene, on the other hand, is a known carcinogen as it may cause fatality if continually exposed to [Nexant's ChemSystems, 2005]. A typical diagram is shown here summarising the reaction mechanism from *n*-butane to maleic anhydride.

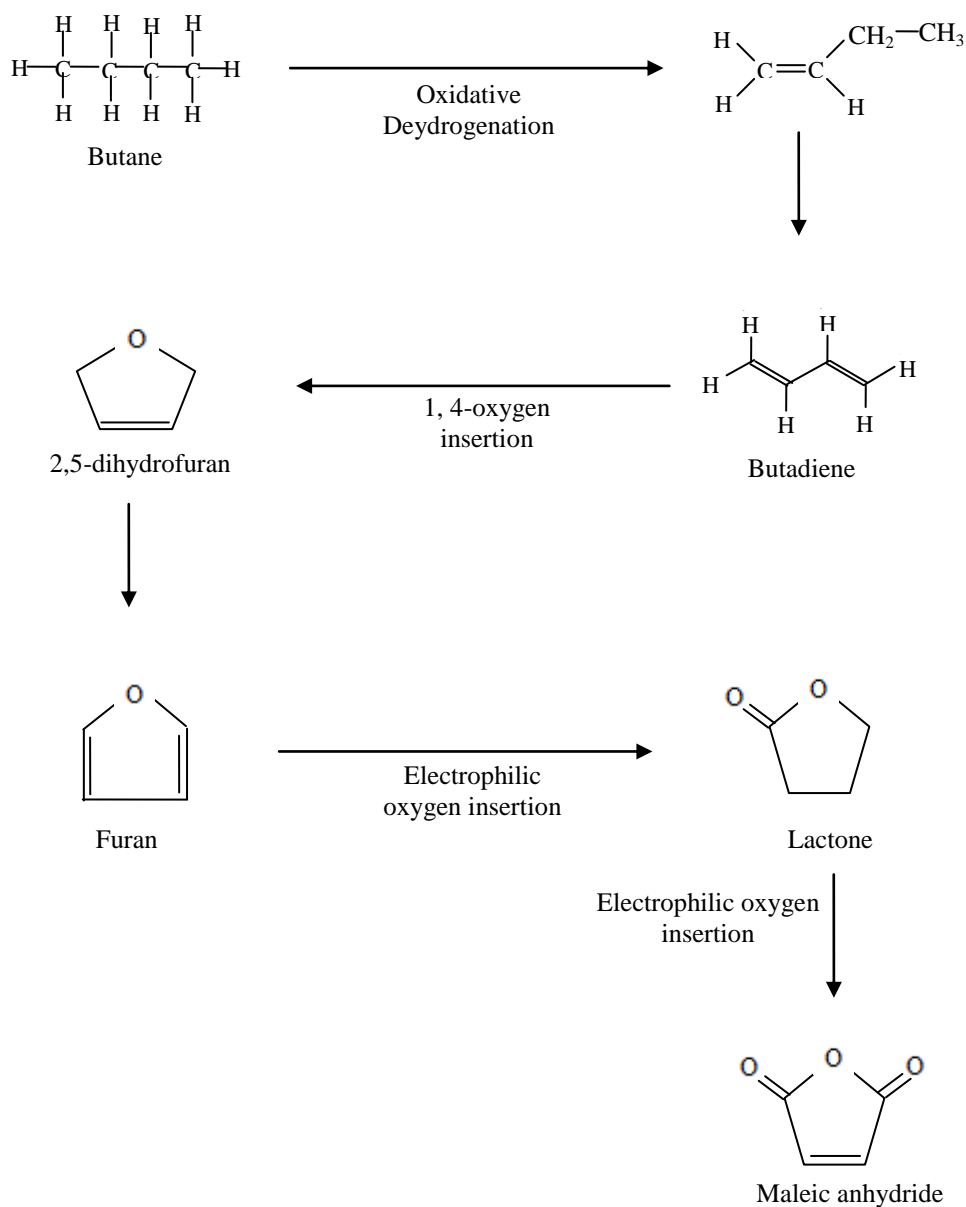


**Figure 2.3: Reaction mechanism from *n*-butane to maleic anhydride**

## CHAPTER 3

## METHODOLOGY AND CHARACTERISATION TECHNIQUES

## 3.1 Materials

Chemicals that were used in the project were the followings:

1. Vanadium (V) pentoxide,  $V_2O_5$  (Merck)
2. *ortho*-Phosphoric acid, *o*- $H_3PO_4$  (85 %) (Merck)
3. 1-butanol,  $CH_3(CH_2)_3OH$  (R & M Chemicals)
4. Iso-butanol,  $CH_3(CH_2)_3OH$  (R & M Chemicals)
5. Nitric acid,  $HNO_3$  (R & M Chemicals)
6. Sulphuric acid,  $H_2SO_4$  (95-98 %) (Merck)
7. Potassium permanganate,  $KMnO_4$  (Fischer Scientific)
8. Ammonium iron (II) sulphate,  $(NH_4)_2Fe(SO_4)_2$  (R & M Chemicals)
9. Potassium nitrate,  $KNO_3$  (R & M Marketing)
10. Benzyl alcohol,  $(C_6H_5)CH_2OH$  (Merck)
11. Hydrochloric acid,  $HCl$  (37 %) (Merck)
12. Acetone,  $CH_3COCH_3$  (Fisher)
13. Diphenylamine,  $Ph_2NH$  (ACROS)
14. Ammonium phosphate,  $NH_4H_2PO_4$  (Merck)
15. Ammonium metavanadate,  $NH_4VO_3$  (Merck)

The gases used were:

1. 1.10 % oxygen in nitrogen (Malaysia Oxygen Berhad (MOX))
2. 99.99% purified nitrogen (Malaysia Oxygen Berhad (MOX))
3. 99.99% purified helium (Malaysia Oxygen Berhad (MOX))
4. 99.99% purified argon (Malaysia Oxygen Berhad (MOX))
5. Liquefied nitrogen gas (Malaysia Oxygen Berhad (MOX))

## **3.2 Methodology**

The parameter that had to be determined in this project was the route of the precursors preparation. The physical and chemical features of the resulted catalysts were compared among the four methods of preparation.

### **3.2.1 Catalysts Preparation via Aqueous Route**

15 g of vanadium pentoxide,  $V_2O_5$  was refluxed together with 200 ml of concentrated HCl (37 %) at 393 K with continuous stirring for 1.5 hour, at which time the solution was dark blue in colour. Ortho-phosphoric acid was added in such a quantity as to obtain the desired P:V atomic ratio. The resulting solution was then heated again to 393 K and maintained under reflux with constant stirring for a further 1.5 hour. The solution was then evaporated to near dryness to a blue-green paste, which was dried in air at 385 K for 16 hour. The resulting green-blue solid was refluxed for 2 hour with distilled water (1 g/20 ml). The suspension was then filtered hot and dried in air at 385 K for 16 hour to give a blue solid, which was the precursor,  $VOHPO_4 \cdot 0.5H_2O$ .

### 3.2.2 Catalysts Preparation via Organic Route

15 g of vanadium pentoxide,  $V_2O_5$  was suspended by rapid stirring into a mixture of 90 ml of isobutyl alcohol and 60 ml of benzyl alcohol. The vanadium oxide - alcohol mixture was then refluxed for 3 hour at 393 K with continuous stirring. The mixture was then cooled to room temperature while continually stirring. Ortho-phosphoric acid was added in such a quantity as to obtain the desired P:V atomic ratio which was 1:1. The resulting solution was then heated again to 393 K and maintained under reflux with constant stirring for 2 hr. The slurry was centrifuged, washed and dried at 353.15 K overnight to obtain the precursor vanadyl hydrogen phosphate hemihydrated,  $VOHPO_4 \cdot 0.5H_2O$ .

### 3.2.3 Catalysts Preparation via Dihydrate Route

10 g of vanadium pentoxide,  $V_2O_5$  was reacted with 60 ml of  $H_3PO_4$  in water under reflux with continuous stirring for 24 hour. The resultant yellow solid was recovered through centrifugation and then washed sparingly with water and over dried at 353.15 K for 16 hour.  $VOPO_4 \cdot 2H_2O$  was then refluxed with isobutanol (1 g/20 ml) for 21 hr and the solid product was recovered by filtration and dried in air at 353.15 K for 16 hour to obtain the precursor,  $VOHPO_4 \cdot 0.5H_2O$ .

### 3.2.4 Catalysts Preparation via Sesquihydrate Route

15 g of vanadium pentoxide,  $V_2O_5$  was first suspended with 90 ml of 85 % of aqueous *ortho*-phosphoric acid, *o*- $H_3PO_4$  in 360 ml of distilled water. The mixture was then stirred under reflux at 393.15 K for 24 hours. The yellow solid ( $VOPO_4 \cdot 2H_2O$ ) obtained after the reflux was then recovered by using centrifuge technique and subsequently washed sparingly with distilled water. Dried sample was obtained after drying it in oven at 353.15 K for overnight.

In the second stage, 10 g of the dried  $\text{VOPO}_4 \cdot 2\text{H}_2\text{O}$  was added to 150 ml of 1-butanol (R & M Chemicals) and refluxed at 353 K for 24 hours. After being cooled to room temperature, a whitish-blue powder was obtained denoted as vanadyl hydrogen phosphate sesquihydrate precursor  $\text{VOHPO}_4 \cdot 1.5\text{H}_2\text{O}$ . The whitish-blue powder was then centrifuged, washed sparingly with acetone and dried overnight in an oven at 353.15 K.

After the precursors had been prepared, they were calcined under a reaction flow of 1.10% oxygen in nitrogen for 24 hours at 733.15 K (460 °C).

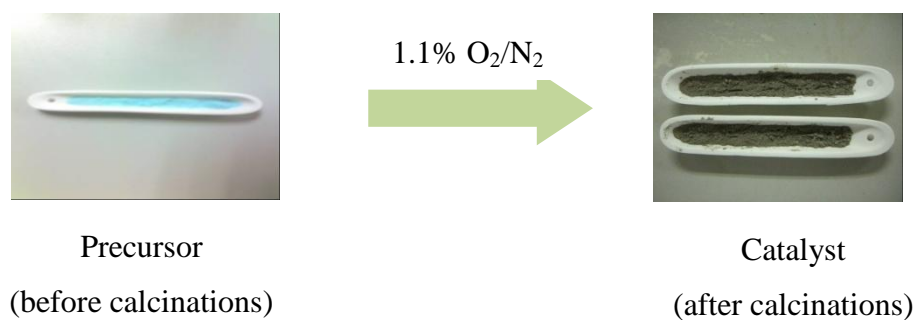


**Figure 3.1: Transformation from precursor to catalyst**

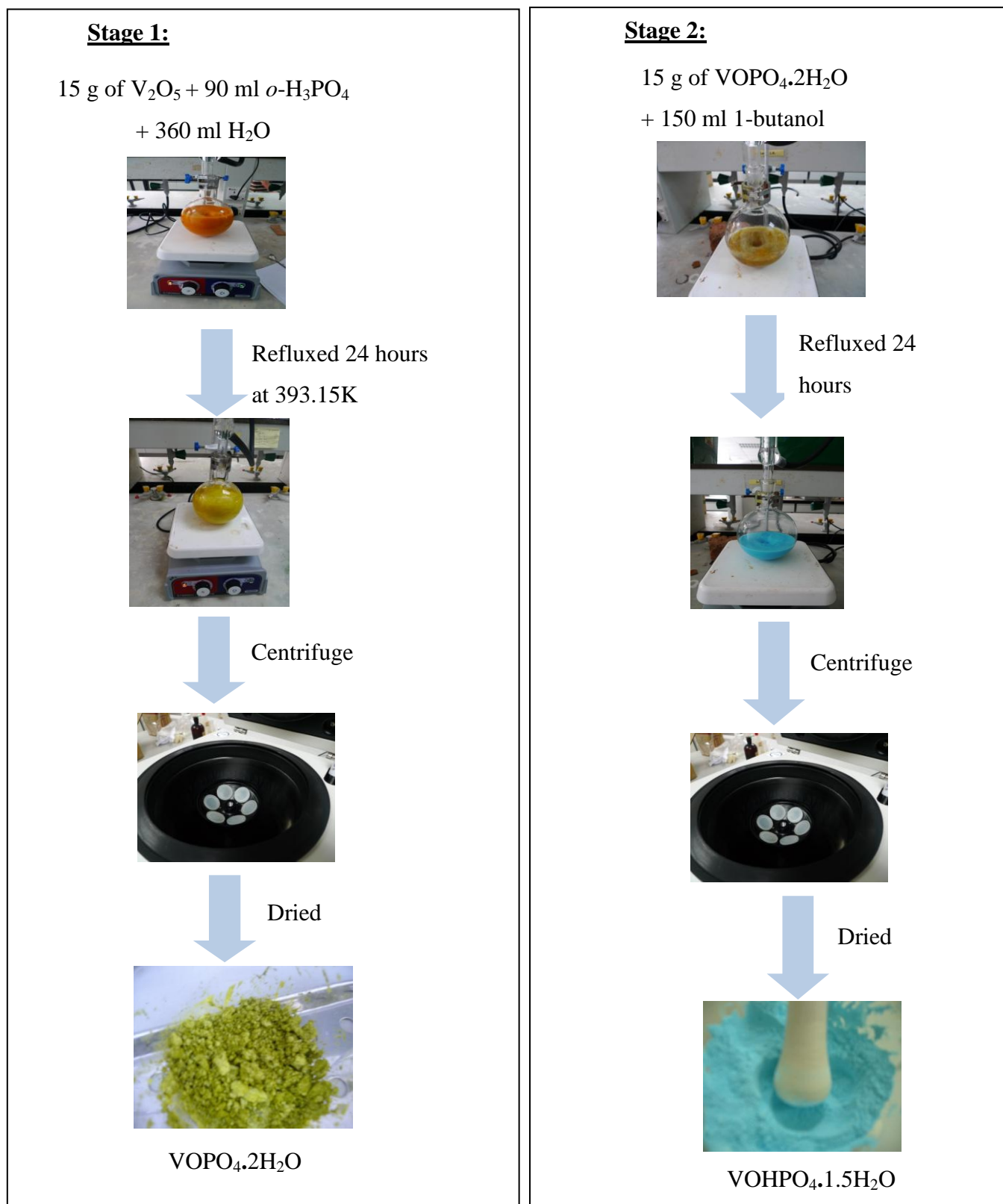


Figure 3.2: Flow diagram of sesquihydrate preparation route

### 3.3 Characterisation Techniques and Instrumentation

#### 3.3.1 X-Ray Diffraction (XRD) Analysis

XRD is an efficient and powerful technique in determining the phase composition of catalysts under ambient temperature and atmospheric pressure. It provides useful information on the qualitative and quantitative analysis of crystalline compounds. XRD serves the two main areas, which are the determination of a solid structure and as a fingerprint characterisation of crystalline materials [Klug and Alexander, 1974].

In 1912, Bragg developed a relationship between the spacing of atomic planes, the angle of diffraction and the wavelength of the incident X-ray. X-rays are diffracted from solids which are crystalline and have regularly repeating atomic structures. XRD method relies upon the particle nature of X-rays to obtain information about the structure of crystalline materials [Klug and Alexander, 1974].

X-rays are produced from an X-ray tube. It is radiated over a crystalline substance and is scattered according to the lattice structure of the solid sample. The scattered X-rays may undergo either destructive or constructive interference and therefore, producing dark dots on a detector plate. If X-rays travel between rows of atoms at the angle of incidence equal to an integral multiple of the wavelength of the incident beam, this would produce 100 % diffraction. On the other hand, d-spacings which are greater or less than the wavelength of the incident X-ray beam will produce a diffracted beam of less than 100 % intensity [Chorkendoff and Niemantsverdriet, 2003] .

Bragg's Law given as:  $n\lambda=2d \sin \theta$  relates the wavelength of the monochromatic X-ray to the diffraction angle and the lattice spacing in crystalline sample [Brag, 1912].

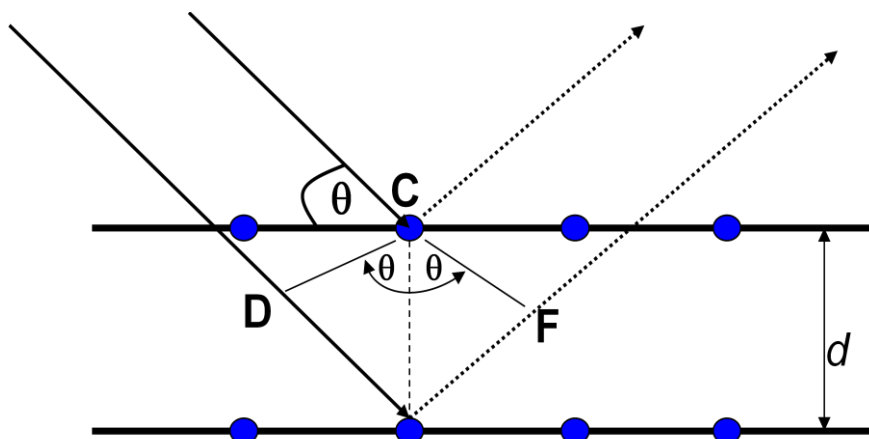


**Figure 3.3: Two X-ray beams directed to parallel crystallographic planes**

Each crystalline solid has its own unique lattice spacing. Hence, the X-rays pattern produced allows the the identification pf crystalline materials. Also, X-ray crystallography may be used to determine its structure for example the packing on the atoms, the interatomic distance and *etc.* For catalysis purpose, XRD also the determines the relative abundance of  $V^{5+}$  and  $V^{4+}$  [Chorkendoff and Niemantsverdriet, 2003].

In addition, the crystallite size can be determined by the XRD method. This is explained by the Debye-Scherrer equation: [Scherrer, 1918].

$$t = \frac{0.89 \lambda}{\beta_{hkl} \cos \theta_{hkl}} \quad (3.1)$$

where

$t$  = crystallite size for  $(h, k, l)$  phase

$\lambda$  = X-ray wavelength of radiation for  $CuK\alpha$

$\beta_{hkl}$  = full-width at half maximum (FWHM) at  $(h, k, l)$  phase

$\theta_{hkl}$  = diffraction angle for  $(h, k, l)$  phase

In this project, the catalyst's diffraction method is obtained from a Shimadzu diffractometer model XRD-6000. The X-rays is generated from a Philip glass diffraction X-ray tube focus 2.7 kW type at ambient temperature. The basal spacing

is determined via powder technique and samples are scanned at the range of  $2\theta = 2^\circ - 60^\circ$  with a scanning rate of  $1.200^\circ \text{ min}^{-1}$ . The diffraction patterns that are obtained are then compared with the Joint Committee on Powder Diffraction Standards (JCPDS) PDF1 database version 2.6 to indentify the catalysts phases [ICDD, 2010].



**Figure 3.4: Shimadzu diffractometer model XRD-6000**

### **3.3.2 BET Multi Point Surface Area Measurement**

Brunauer-Emmett-Teller (BET) multi point analysis is used to determine the specific surface area by physical adsorption of a gas on the surface of the solid and by calculating the amount of adsorbate gas corresponding to a monomolecular layer on the surface. Physical adsorption results from relatively weak forces (van der Waals forces) between the adsorbate gas molecules and the adsorbent surface of a test powder. The analysis is usually carried at the temperature of liquid nitrogen. The amount of gas adsorbed can be measured by a volumetric or continuous flow procedure.

In this project, a Sorptomatic 1990 which is based on the volumetric principle was used. It can perform both physisorption and chemisorptions. The physisorption of nitrogen gas allows the determination of properties like porosity, strength,

hardness, permeability, separation selectivity, corrosion and thermal stress resistance. These properties in turn can be correlated to the porosity of the material. Chemisorption provides information on the quality, activity, and selectivity of the catalysts.



**Figure 3.5: Thermo Finnigan Sorptomatic 1990**

The catalysts powders were heated and degassed overnight in a flow of helium gas to remove any adsorbed foreign molecules prior to analysis. During the analysis, the sample was placed inside a vacuum chamber at a constant temperature of liquid nitrogen. The sample was then subjected to a wide range of pressures in order to generate adsorption/desorption isotherms.

The adsorption isotherm of the BET technique is given as [Braunauer *et al.*, 1938]

$$\frac{1}{V_a \left( \frac{P_0}{P} \right) - 1} = \frac{C-1}{V_m C} \times \frac{P}{P_0} + \frac{1}{V_m C} \quad (3.2)$$

where

$P$  = partial vapor pressure of adsorbate gas in equilibrium with the surface at 77.4 K (b.p of liquid nitrogen), in pascals

$P_o$  = saturated pressure of adsorbate gas, in pascals,  $T$  = temperature, K

$V_a$  = volume of gas adsorbed at standard temperature and pressure (STP) [273.15 K and atmospheric pressure ( $1.013 \times 10^5$  Pa)], in millilitres,

$V_m$  = volume of gas adsorbed at STP to produce an apparent monolayer on the sample surface, in millilitres,

$C$  = dimensionless constant that is related to the enthalpy of adsorption of the adsorbate gas on the powder sample

### 3.3.3 Redox Titration

This method was previously developed by Miki Niwa and Yuichi Murakami (1982) on the investigation of ammoxidation of toluene on  $V_2O_5/Al_2O_3$ . In this project however, redox titration was carried out to determine the vanadium valence (AV) of the V-P-O catalysts and/or to obtain the average oxidation state of vanadium. Firstly, a known amount of sample catalyst was dissolved in 100 ml sulphuric acid (2M). It was then cooled to room temperature before being titrated with potassium permanganate solution to  $V^{5+}$ . The end point was determined when the colour changed from original greenish blue to pink. The volume of potassium permanganate used was given as  $V_1$ . Then, the oxidised solution was treated with ammonia iron (II) sulphate solution (0.01M) to reduce  $V^{5+}$  to  $V^{4+}$ . For this titration, diphenylamine was used as an indicator. End point was reached when the original purple colour disappeared and become colourless. The volume of ammonia iron (II) sulphate used was recorded as  $V_2$ .

Next, another fresh 25 ml from the original solution was then titrated with 0.01 N ammonium iron (II) sulphate solution. Diphenylamine was still used as an indicator here. This is to determine the  $V^{5+}$  in the original solution. The end point was reached when the solution changes from purple to greenish blue. The volume of ammonium iron (II) sulphate solution used was recorded as  $V_3$ .

Equation below was used to determine the average oxidation number of vanadium (AV) [Niwa and Murakami, 1982]:

$$AV = \frac{5V^{5+} + 4V^{4+} + 3V^{3+}}{V^{5+} + V^{4+} + V^{3+}} \quad (3.3)$$

where

$V^{5+}, V^{4+}, V^{3+}$  = concentration of vanadium at different oxidation state.

In order to obtain the separate values of  $V^{5+}$ ,  $V^{4+}$ , and  $V^{3+}$ , the following equations are used:

$$V^{3+} = 20(0.01)V_1 - 20(0.01)V_2 + 20(0.01)V_3 \quad (3.4)$$

$$V^{3+} = 20(0.01)V_1 - 20(0.01)V_2 + 20(0.01)V_3 \quad (3.5)$$

$$V^{3+} = 20(0.01)V_1 - 20(0.01)V_2 + 20(0.01)V_3 \quad (3.6)$$

where

$V_1$  = volume of potassium permanganate used

$V_2, V_3$  = volume of ammonium iron (II) sulphate

### 3.3.4 Scanning Electron Microscopy (SEM)

SEM uses electrons to produce an image in order to obtain information such as morphology and crystallographic order of the sample. Thus, it also provides the length of the catalyst particles. A metallic filament at the top of the microscope acting as a cathode is heated to produce a stream of electrons. It is then accelerated by means of a positive electric potential to follow a vertical path through the column of the microscope.

This beam of electrons is then directed and passed through electromagnetic lenses which then resulted into a thin, focused and monochromatic beam that hits the sample. Once the beam hits the sample, interactions occur inside and ejecting other electrons (backscattered and secondary) from the sample. Detectors on the other hand collect these electrons and convert them to a signal, producing an image.

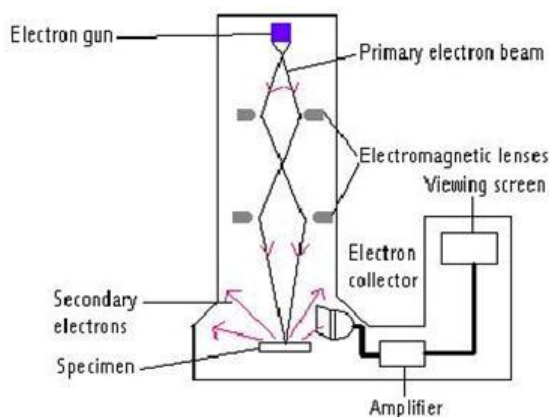


**Figure 3.6: Scanning electron microscopy**

In this project, the model Hitachi S4300N was used. For SEM analysis, a small amount of catalysts samples were used. The catalysts powder were first coated with a thin layer of gold metal at the surface for conductive purposes during the analysis. Then, a beam of electrons scanned across the surface of the catalysts. Interaction between the beam and the sample resulted in the emission of the electrons and photons, as the electrons penetrated the surface of the catalysts. Following this, the emitted particles were then collected and sent to the detector to provide information regarding the surface morphology.



**Figure 3.7: Hitachi S4300N**

### **3.3.5 Energy Dispersive X-Ray (EDX)**

The EDX analysis always works together scanning electron microscope which is used to identify the elemental composition of the catalyst. The EDX analysis uses the electron beam in the SEM to bombard on the catalyst atoms' own electrons. Some of the inner shell electrons will be knocked off and the vacancy of it will then be replaced by a higher energy electron from an outer shell. Transferring the outer electron will emit some energy in the form of X-Ray and the amount of energy release is unique for each element present. Thus, the atoms can be identified by measuring the amount of energy present in the X-Ray.

The output of an EDX analysis is an EDX spectrum which is a plot of how frequently an X-Ray is received for each energy level. Since every element have its own X-Ray characteristic, each of the peak present indicates the corresponding element. A higher peak in the spectrum means the more concentrated of the element is in the sample.

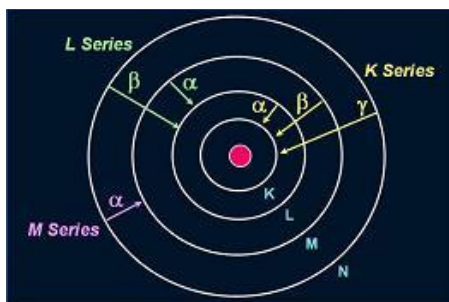


**Figure 3.8: Shells that may present in an atom**

Not only does the EDX spectrum identifies the element from the peak, but also the type of X-Ray to which it corresponds as well. For example (as shown in Figure 3.4), X-Ray emitted by an electron falling from L-shell to K-shell is identified as K-alpha peak.

Similar to SEM, EDX analysis used a small amount of catalysts samples. During the analysis, atoms on the surface of the catalysts powders were excited by the electron beam from SEM, emitting specific wavelengths which were characteristic of the atomic structure of the sample.

### 3.3.6 Inductively Coupled Plasma Optical Emission Spectrometry (ICP-OES)

The analytical principle used in the ICP-OES systems is the optical emission spectroscopy. The ICP torch consists of three concentric quartz tubes made of glass. When the torch is turned on, a coil with create an intense magnetic field within in causing the argon gas to be ignited. Once it is ignited, ionization process begins.

The temperature of the plasma can rise up to 700 K as a result of the inelastic collisions created between the neutral argon atoms and the charged particles. When sample is introduced directly into the plasma flame, the sample with collide with other electrons and ions causing itself broken down charged ions as well. The various molecules break up into their respective atoms which then lose electrons and

recombine repeatedly in the plasma emitting radiations with respective wavelengths of each element.

The radiation emitted can be passed to the spectrometer optics, where it is dispersed into its spectral components. With this optical chamber, the radiation consists of separate colors fall upon an array of semiconductor photodetectors such as CCD (charge coupled device).

In this project, the model Perkin-Elmer Emission Spectrometer Model Plasma was used to determine the phosphorus/vanadium ratios. Catalysts samples were digested in aqueous nitric acid to release the metal elements into solution for analysis. The two elemental standards (phosphorus and vanadium) were prepared in the 10 to 50 ppm concentration range. The actual concentrations of these two elements in the sample catalysts were determined from this range of standards using the calibration graphs obtained from the elemental standards.

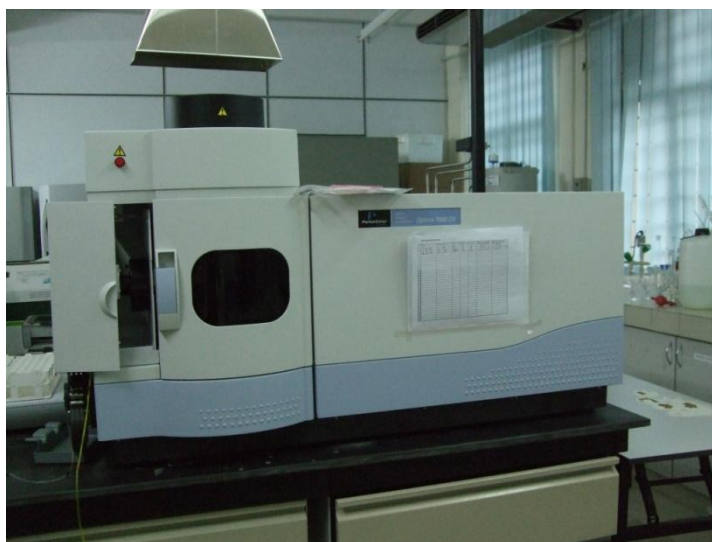


**Figure 3.9: Perkin-Elmer Emission Spectrometer Model Plasma**

## CHAPTER 4

### RESULTS AND DISCUSSION

#### 4.1 Introduction

In this research, four samples of vanadium phosphate oxide (V-P-O) catalysts were prepared using different methods: (i) Aqueous route (VPA), prepared by using the standard aqueous hydrochloric acid, HCl; (ii) Organic route (VPO) prepared by the reaction of vanadium pentoxide,  $V_2O_5$  with *ortho*-phosphoric acid,  $H_3PO_4$  in a mixture of isobutanol and benzyl alcohol; (iii) Dihydrate route (VPD), prepared by the reaction of  $VOPO_4 \cdot 2H_2O$  with isobutanol; and (iv) Sesquihydrate route (VPS), prepared by the reaction of  $VOPO_4 \cdot 2H_2O$  with 1-butanol. The effects of the different preparation routes towards the physicochemical properties were characterised and examined. The corresponding precursors were denoted as VPAP, VPOP, VPDP, and VPSP. Except VPSP, all the other precursors like VPAP, VPOP and VPDP comprised of the phase, vanadyl hydrogen phosphate hemihydrate ( $VOHPO_4 \cdot 0.5H_2O$ ). The sesquihydrate route on the other hand had observed the phase of vanadyl hydrogen phosphate sesquihydrate ( $VOHPO_4 \cdot 1.5H_2O$ ). The corresponding V-P-O catalysts were obtained by calcining the precursors at 733 K in a flow of 1.1% oxygen/nitrogen for 24 hours. These catalysts were denoted as VPA24, VPO24, VPD24, and VPS24.

## 4.2 X-Ray Diffraction Analysis

The XRD patterns of the precursors VPAP, VPOP, and VPDP showed characteristic peaks of vanadyl hydrogen phosphate hemihydrate ( $\text{VOHPO}_4 \cdot 0.5\text{H}_2\text{O}$ ) with reflections observed at  $2\theta = 15.5^\circ$ ,  $19.6^\circ$ ,  $24.14^\circ$ ,  $27.0^\circ$ , and  $30.4^\circ$  [Volta and Acad, 2000]. The three main characteristic peaks at  $2\theta = 15.5^\circ$ ,  $27.0^\circ$ , and  $30.4^\circ$  correspond to the planes (0 0 1), (1 2 1), and (2 2 0) respectively as shown in Figure 4.1. On the other hand, the XRD pattern of the precursor VPSP showed the characteristic reflection of vanadyl hydrogen phosphate sesquihydrate ( $\text{VOHPO}_4 \cdot 1.5\text{H}_2\text{O}$ ). A similar XRD pattern of this precursor was reported by Taufiq-Yap and co-workers in year 2004. Comparing all the precursors, the one obtained via aqueous method gave the highest crystallinity with an outstanding development of diffraction peak at  $2\theta = 15.5^\circ$ . Precursors using organic alcohols as reducing agents (VPOP, VPDP, and VPSP) were less crystalline.

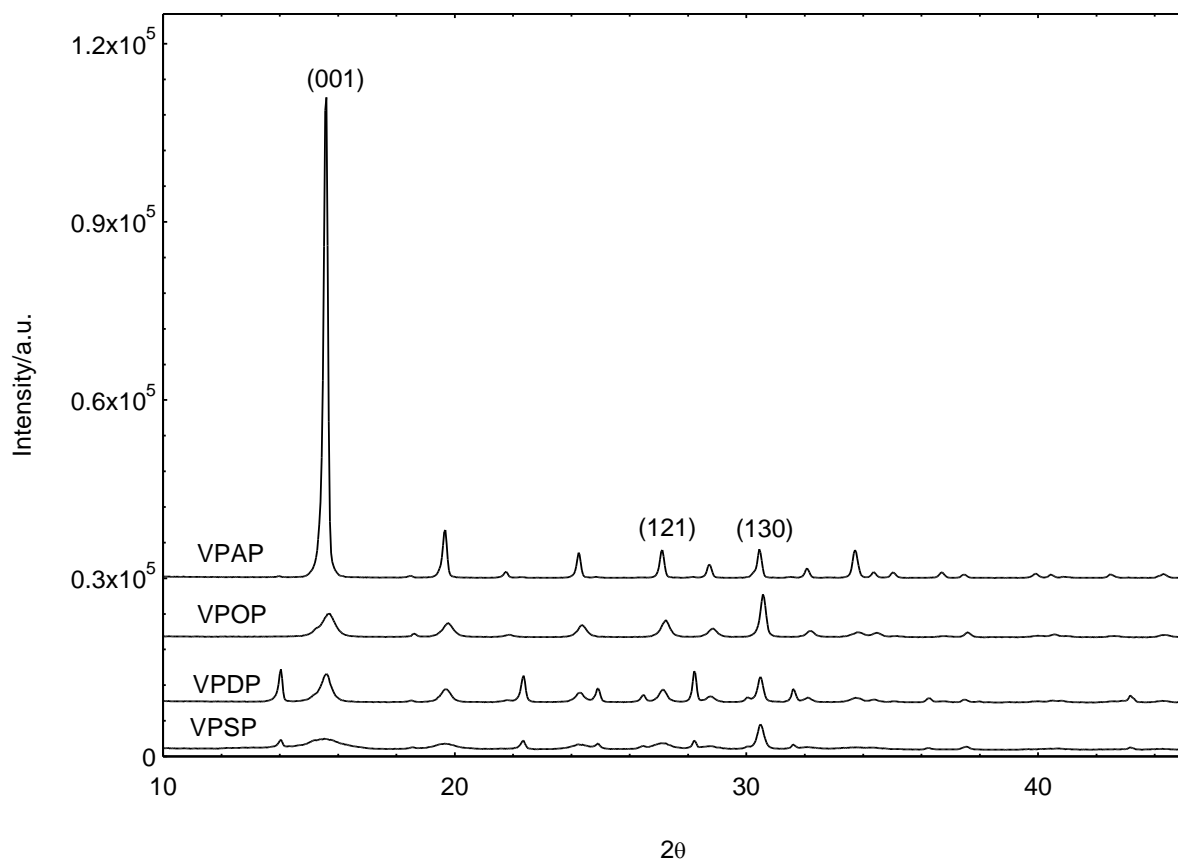


**Figure 4.1: XRD patterns of precursors VPAP, VPOP, VPDP, and VPSP**

Figure 4.2 showed the diffractogram of the catalysts having calcined in 1.1% oxygen in nitrogen balance for 24 hours. Although from different precursors, the XRD profiles of the catalysts show similar diffraction patterns of well crystallized vanadyl pyrophosphate,  $(VO)_2P_2O_7$  phases. Three main characteristic peaks appeared at  $2\theta = 22.8^\circ$ ,  $28.4^\circ$ , and  $29.8^\circ$  are corresponded to the planes (0 2 0), (2 0 4) and (2 2 1), respectively. There are two types of phases appeared in the catalysts which are  $(VO)_2P_2O_7$  (JCPDS File No. 34 -1381) and  $\beta$ - $(VO)_2P_2O_7$  (JCPDS File No. 34-1247) at which  $\beta$ - $(VO)_2P_2O_7$  phase being the major component. Overall, the catalysts possessed lower crystallinity as compared to their corresponding precursors. Among the four catalysts, VPA24 had the highest crystallinity. This was due to its highly crystalline precursor. VPA24 showed an outstanding development of diffraction peak at  $2\theta = 22.8^\circ$ , which corresponded to the development of (0 2 0) plane. This result suggested that the dominant surface of VPA24 was composed of (1 0 0) layer. Centi (1993) claimed that the (0 2 0) plane is active for the selective oxidation of *n*-butane. For the other catalysts such as VPO24, VPS24, and VPD24, the most intense peak is observed at  $2\theta = 28.4^\circ$  or the (2 0 4) plane suggesting that the surfaces of these catalysts were dominated by the (0 1 1) layer [Taufiq-Yap and Saw, 2008].

Crystallite size of the catalyst can be calculated using the Debye-Scherrer equation given as:

$$t (\text{\AA}) = \frac{0.89\lambda}{FWHM \times \cos\theta} \quad (4.1)$$

where

$t$	=	crystallite size for ( $h k l$ ) plane in unit $\text{\AA}$
$\lambda$	=	X-ray wavelength of radiation for $CuK\alpha$
FWHM	=	Full width at half maximum at the ( $h k l$ ) plane
$\theta$	=	Diffraction angle at ( $h k l$ ) plane

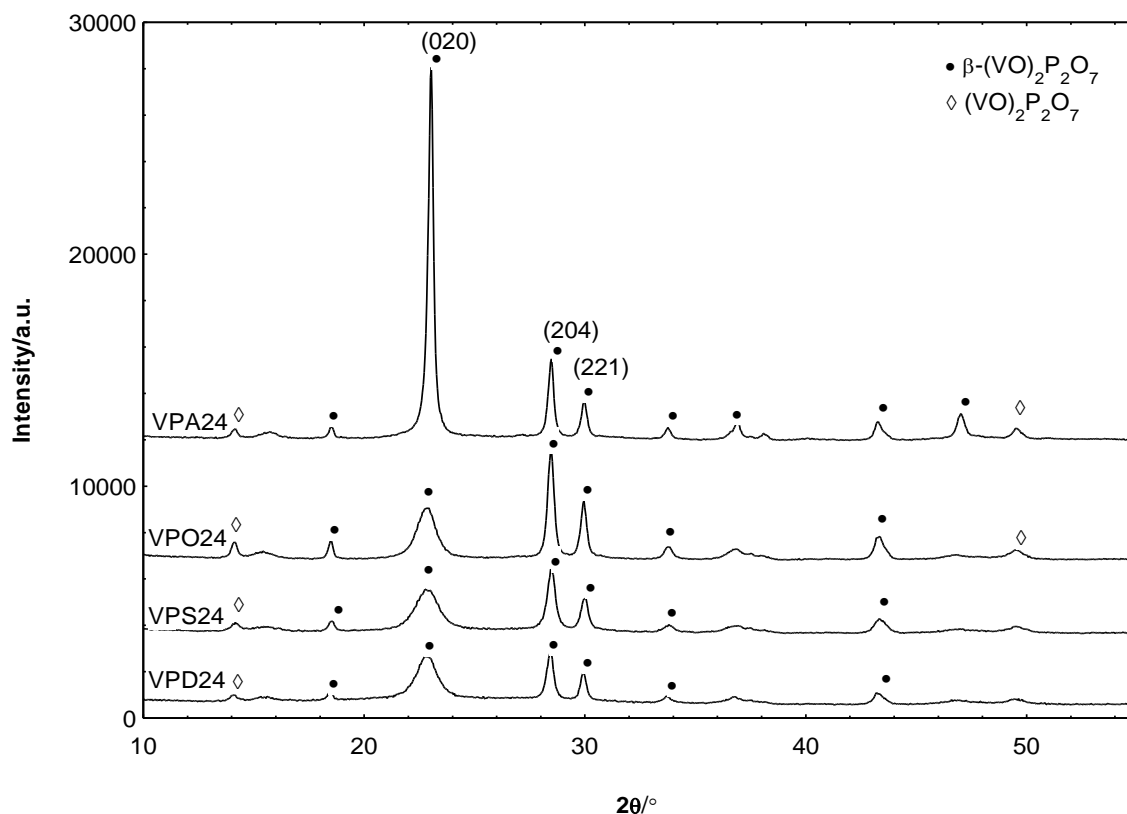


**Figure 4.2: XRD patterns of VPA24, VPO24, VPD24, and VPS24 catalysts**

The crystallite size is always inversely proportional to the FWHM. According to Taufiq-Yap *et al.* (2004), the FWHM at (0 2 0) plane indicates the crystallite size in the (1 0 0) direction. Since the oxidation of  $(VO)_2P_2O_7$  catalyst starts at the side faces of the (1 0 0) plane as proposed by Centi and Trifiro (1992), the half width of the (0 2 0) plane is used to determine the crystallite size of the catalysts. The calculated crystallite size of (0 2 0) plane for VPA24, VPO24, VPD24, and VPS24 were 326.64 Å, 76.73 Å, 93.51 Å, and 71.56 Å respectively. The crystallite size of (2 0 4) plane for these catalysts were calculated as 330.33 Å, 131.44 Å, 270.82 Å, and 144.20 Å. VPA24 had comparably larger crystallite size among all. It was predicted that large crystallite would have a smaller specific surface area and a lower catalytic activity. However, apart from the crystallite size, there are also other factors that contribute to the total surface area. This will be discussed in the later section.

**Table 4.1: XRD data of V-P-O catalysts.**

Catalysts	Linewidth <sup>a</sup> (0 2 0) (°)	Linewidth <sup>b</sup> (2 0 4) (°)	Crystallite Size <sup>c</sup> (0 2 0) (Å)	Crystallite Size <sup>c</sup> (2 0 4) (Å)
VPA24	0.00482	0.00481	326.63	330.33
VPO24	0.01682	0.00587	76.73	131.44
VPD24	0.02050	0.01210	93.51	270.82
VPS24	0.02198	0.01103	71.56	144.20

<sup>a</sup> FWHM of (020) reflection plane

<sup>b</sup> FWHM of (204) reflection plane

<sup>c</sup> Crystallite size by means of Scherrer's equation.

### 4.3 BET Multipoint Surface Area Measurements

The BET surface area measurements were carried out using the nitrogen adsorption-desorption application at 77 K, which is the temperature of liquid nitrogen. The specific surface area for VPA24, VPO24, VPD4 and VPS24 were 6.232 m<sup>2</sup> g<sup>-1</sup>, 26.638 m<sup>2</sup> g<sup>-1</sup>, 9.919 m<sup>2</sup> g<sup>-1</sup> and 12.335 m<sup>2</sup> g<sup>-1</sup>, respectively. Catalyst prepared via aqueous route had the smallest surface area as expected from its large crystallite size. However, this was not the case for VPO24 (76.73 Å) because though it has a larger crystallite size compared to VPS24 (71.56 Å), the specific surface area of VPO24 was doubled the VPS24. This could be explained by other factors that may lead to the increment of the total surface area. For example, the total surface area could be affected by the catalysts' porosity, the amount of platelets present in the V-P-O crystalline structure as well as the degree of isolation for the platelets. It was also expected that catalyst with high surface area would have more split (VO)<sub>2</sub>P<sub>2</sub>O<sub>7</sub> whereas catalyst that has low surface area will have bigger size of crystal platelets. Surface area is a very important characteristic of catalyst because higher surface area indicates a higher catalytic activity. However, this is also very much dependent on the relative exposure of (0 2 0) planes, which is responsible for the catalytic activity

[Ruiz and Delmon, 1987]. The results on the specific surface area obtained in this study are in agreement with those reported by Hutching *et al.* (1998). Though from both studies, VPA was shown to have the lowest surface area while VPO having the highest surface area, the values obtained are significantly different. This might be due to the different calcination environment whereby in this study, the precursors were calcined under the flow of 1.1% O<sub>2</sub>/N<sub>2</sub> rather than *n*-butane in air mixtures. From their study also, the adsorption isotherms encountered for all the catalysts were of Type II indicating the presence of mesopores with pore size varies from 2 nm to 50 nm [Sing *et al.*, 1985].

**Table 4.2: BET surface area analysis of V-P-O catalysts**

Catalysts	Specific surface area (m <sup>2</sup> g <sup>-1</sup> )
VPA24	6.232
VPO24	26.638
VPD24	9.919
VPS24	12.335

#### 4.4 Chemical Analysis

##### 4.4.1 Chemical Compositions

The bulk P/V ratios of the catalysts were determined using the ICP-OES. The bulk P/V ratios of the catalysts were as follows: 1.138 for VPA24, 1.083 for VPO24, 1.104 for VPD24 and 1.030 for VPS24. Comparing to the EDX analysis, the surface P/V ratios of the catalysts were slightly higher than their bulk ratios (Table 4.3). The results showed that there was excess phosphorus present in the catalyst with respect to the chemical formula of vanadyl pyrophosphate. This excess phosphate was strongly bound to the surface and cannot be removed by simply washing of the precursor in polar solvents [Gulians and Carreon, 1991]. It had been proposed by several scientific literatures that a slight excess of phosphorus (P/V atomic ratio from 1.05 to 1.1) is necessary for obtaining high catalytic performance. Cavani and Trifiro (1994) proposed that this excess phosphorus present in the precursor helps to

stabilize  $(VO)_2P_2O_7$  against overoxidation in oxygen containing atmosphere such that it prevents the bulk oxidation of  $(V^{IV}O)_2P_2O_7$  to the  $V^VOPO_4$ . The excess phosphate terminates the side faces of the (0 2 0) plane of  $(VO)_2P_2O_7$  in the form of the surface  $VO(PO_3)_2$  phase, which prevents the oxidation of vanadyl pyrophosphate due to the lower oxidizability of  $VO(PO_3)_2$  [Matsuura and Yamazaki, 1990]. In 1991, Cornaglia and co-workers found out that the excess phosphorus is localized at the surface of vanadyl pyrophosphate catalysts (surface P/V = 1.5 – 3.0), which explained why surface P/V ratio is always higher than the bulk ratio. The P/V atomic ratios for all the samples obtained are between 1.03 and 1.30.

**Table 4.3: Chemical compositions and average oxidation numbers of vanadium for V-P-O Catalysts**

Catalysts	ICP	EDX	Average oxidation numbers of vanadium		
			$V^V$ (%)	$V^{IV}$ (%)	$V_{av}$
VPA24	1.138	1.300	19.15	80.85	4.1915
VPO24	1.083	1.122	14.86	85.14	4.1486
VPD24	1.104	1.180	19.55	80.45	4.1955
VPS24	1.030	1.091	19.24	80.76	4.1924

#### 4.4.2 Oxidation State of Vanadium

The bulk average oxidation states of all four catalysts were determined using volumetric titration. The average oxidation states obtained were 4.1915, 4.1486, 4.1924 and 4.1955 for VPA24, VPO24, VPS24 and VPD24, respectively. The breakdown of  $V^{4+}$  and  $V^{5+}$  composition are summarized in Table 4.3. The presence of  $V^{5+}$  in all the catalysts indicated that  $VOPO_4$  phase did exist. However, this corresponding phase was not detected by the XRD. This had been a limitation of the XRD whereby it was not sensitive enough to detect the low concentration of  $VOPO_4$  in  $(VO)_2P_2O_7$ . According to Cavani *et al.* (2000), there might be as high as 20% of  $VOPO_4$  in addition to  $(VO)_2P_2O_7$  with no clear modification of the XRD pattern.

During the calcination at high temperature,  $V^{4+}$  was oxidized to  $V^{5+}$  in the presence of oxygen. Cheng and Wang (1996) reported that the reduced species ( $V^{4+}$  and  $V^{3+}$ ) appeared to have high surface area and the  $(VO)_2P_2O_7$  may act to disperse  $V^{5+}$  species. However, as the V-P-O catalyst was overoxidized, the abundance of the reduced species would correspondingly decrease and the crystallization of  $V^{5+}$  species occurred. Hence, when the abundance of  $V^{5+}$  increases, the surface area will decrease due to crystallization. This was observed in the results whereby VPD24 had the highest vanadium valence which was associated with a lower specific surface area compared to VPO24 and VPS24.

## 4.5 Scanning Electron Microscopy

All four catalysts prepared from different routes resulted in different surface morphologies.

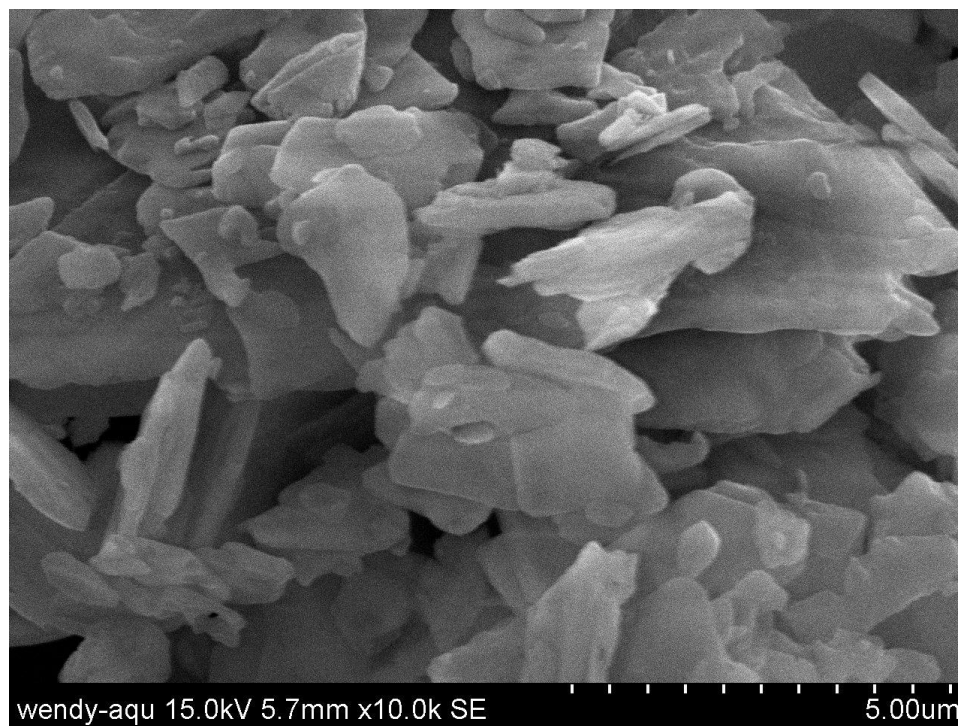


**Figure 4.3: SEM micrographs of VPA24**

VPA24 showed simple shape of large and thick platelets. This was in good agreement with the result obtained from XRD patterns that the crystallite size was the largest for VPA24. The platelets were found to stack together decreasing the specific surface area.

VPO24 (Figure 4.4), on the other hand, consisted of crystal plates with smooth surface arranged into rosette shaped clusters. According to Hutchings *et al.* (1998), these rosette-shape clusters are made up of  $(VO)_2P_2O_7$  platelets that preferentially exposes the (0 2 0) crystal plane. From the SEM micrograph, VPO24 was observed to have more splits between the platelets.



**Figure 4.4: SEM micrographs of VPO24**

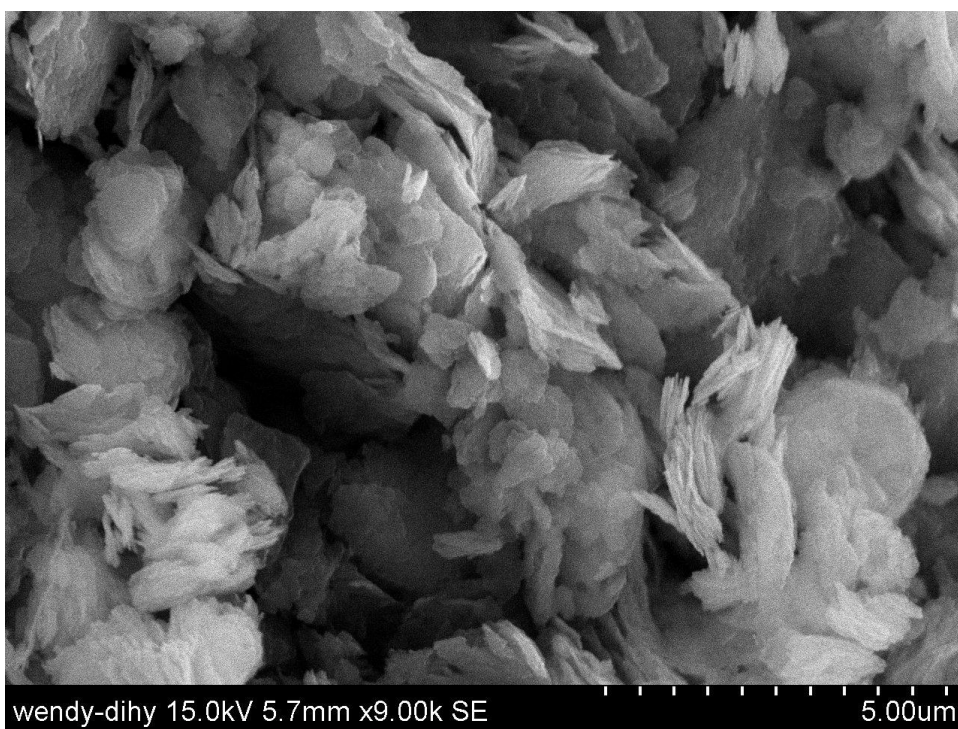


**Figure 4.5: SEM micrographs of VPD24**

From Figure 4.5, VPD24 showed no rosette shape like VPO24. Instead, the catalyst appeared to be comprised of small and round platelets that were closely packed to each other. There was also less splits observed in VPD24 that explained its low surface area.



**Figure 4.6: SEM micrographs of VPS24**

As shown in Figure 4.6, VPS24 also showed the structure of rosette-shape clusters consisting plate-like crystals. Similarly, this catalyst preferentially exposes the (0 2 0) crystal plane [Hutchings *et al.*, 1998]. In addition, there was a unique feature about VPS24 that some of the edges were found to be folded which could not be observed for other synthesised catalysts via different routes.

## CHAPTER 5

### CONCLUSIONS AND RECOMMENDATIONS

#### 5.1 Conclusions

In this study, the effects of different preparation routes on the physicochemical properties were examined. From all the routes other than sesquihydrate route, the precursors comprised of the same phase, which was the vanadyl hydrogen phosphate hemihydrates. As for sesquihydrate route, the precursor was the vanadyl hydrogen phosphate sesquihydrate. Though different phases were obtained, all the four precursors had successfully transformed into vanadyl pyrophosphate catalysts with similar characteristic peaks found in XRD analysis.

Catalyst prepared from the aqueous route showed the highest crystallinity. In contrast, catalysts prepared from alcohols reduction showed lower crystallinity. From BET surface area measurements, catalyst from organic route showed the highest specific surface area followed by sesquihydrate, dihydrate and aqueous catalysts.

P/V atomic ratios for all the four catalysts were found in between the optimal values (1.01 – 1.30). Also, results from redox titration showed that there were a little of the  $V^{5+}$  phase in the catalyst however was not detected by XRD. The vanadium valence is lowest for organic route catalyst followed by aqueous, sesquihydrate and dihydrate route.

Catalyst prepared from aqueous route showed large and thick platelets. On the other hand, catalysts prepared via organic and sesquihydrate route had shown

similar structures resembling a rosette-shape clusters consisted of various sizes of crystal platelets. As for dihydrate route catalyst, it appeared to be small and round platelets that were packed to each other.

## 5.2 Recommendations

It is recommended that the catalysts produced be tested in the catalytic oxidation of *n*-butane to maleic anhydride. This can be done by using a catalytic reactor at which the gases *n*-butane and air are fed to the reactor with a composition of 1% *n*-butane in air. An on-line gas chromatograph is used to analyse the composition of the products.

With the results on catalytic activity and selectivity obtained, one will be able to justify the catalysts' activity and selectivity with respect to their physicochemical properties.

From this research, the catalyst synthesised via organic route had the most prominent results among all. Hence, metal promoters should be incorporated into it as to determine the effects of promoters on the chemical and physical aspects of the catalyst.

## REFERENCES

- Abon M. and Volta J. C. (1997). Vanadium phosphorus oxides for *n*-butane oxidation to maleic anhydride. *Applied Catalysis. A General*, 157, 173 – 193.
- Bond G. C. (1987). *Basic principles of catalysts: Heterogeneous catalysis: Principles and applications*. 2<sup>nd</sup> Edition. Clarendon Press, Oxford.
- Bursca G., Cavani F., Trifiro F. and Centi (1986). Nature and mechanism of formation of vanadyl pyrophosphate: Active phase in *n*-butane selective oxidation. *Journal of Catalysis*. 99, 400 – 414.
- Cavani F., Centi G. and Trifiro F. (1984). Catalyzing butane oxidation to maleic anhydride. *Applied Catalysis*, 24, 18 – 25.
- Centi G. (1993). Vanadyl pyrophosphate catalysts. *Catalysis Today*. 16, 1 – 5.
- Centi G., Cavani F. and Trifiro F. (2001). *Selective Oxidation of Heterogeneous Catalysis. Fundamental and Applied Catalysis*. Kluwer Academic/Plenum Publishers, New York.
- Centi G., Trifiro F., Ebner J. R. and Franchetti V. M. (1988). Mechanistic aspect of maleic anhydride synthesis from C4 hydrocarbons over phosphorus vanadium oxide. *Chemical Review*, 88, 50 – 80.
- Cheng W. H. and Wang W. (1996). Effect of calcinations environment on the selective oxidation of *n*-butane to maleic anhydride over promoted and unpromoted VPO catalysts. *Applied Catalysis. A General*, 156, 57 – 69.
- Chorkendoff I. And Niemantsverdriert J.W. (2003). *Introduction to Catalysis in: Concepts of Modern Catalysis and Kinetics*. WILEY-VCH. N6.
- Cornaglia L. M., Caspani C. and Lombardo E. A. (1991). Physicochemical characterization and catalytic behaviour of VPO formulations. *Applied Catalysis*, 74, 15 – 20.
- Ebner J. R. and Thompson M. R. (1991). In *Structure Acidity and Selectivity Relationships in Heterogeneous Catalysis*. Eds Elsevier, Amsterdam.

- Ebner J. R. and Thompson M. R. (1993). An active site hypothesis for well-crystallized vanadium phosphorus oxide catalyst systems. *Catalysis Today*, 16, 51 – 60.
- Garbassi F., Bart J. C. J., Tassinari R., Vlaic G. and Lagarde P. (1985). Catalytic *n*-Butane Oxidation Activity and Physicochemical Characterization of Vanadium Phosphorus Oxides with Variable P/V Ratio. *Journal of Catalysis*, 98, 317 – 325.
- Hammett L. P. (1970). *Physical Organic Chemistry*. McGraw Hill, New York: Chapter 9.
- Hinshelwood C. N. (1940). *The Kinetics of Chemical Change*. Clarendon Press, Oxford.
- Hodnett B. K. and Delmon B. (1984). Influence of the phosphorus/vanadium ratio on the solid state chemistry and redox properties of vanadium-phosphorus based catalysts. *Journal of Catalysis*, 88, 43 – 53.
- Hucknall D. J. (1974). *Selective Oxidation of Hydrocarbons*. Academic Press, London.
- Hutchings G. J. (1991). Effect of promoters and reactant concentration on the selective oxidation of *n*-butane to maleic anhydride using vanadium phosphorus oxide catalysts. *Applied Catalysis*, 72, 1 – 32.
- Hutchings G. J. and Higgins R. (1996). Effect of promoters on the selective oxidation of *n*-butane with vanadium phosphorus oxide catalysts. *Journal of Catalysis*, 162, 153 – 168.
- Hutchings G. J., Kiety C. J., Sananes – Schulz M. T., Burrows A. and Volta J. C. (1998). Comments on the nature of the active sites of vanadium phosphorus catalysts for butane oxidation. *Catalysis Today*, 40, 273 – 286.
- Hutchings G. J., Sananes M. T., Sajip S., Kiely C. J., Burrows A., Elison I. J. and Volta J. C. (1997). Improved method of preparation of vanadium phosphate catalysts. *Catalysis Today*, 33, 161 – 171.
- Ishimura T., Sugiyama S. and Hayashi H. (2000). Vanadyl hydrogen phosphate sesquihydrate as a precursor for preparation of  $(VO)_2P_2O_7$  and cobalt-incorporated catalysts. *Journal of Molecular Catalysis: A Chemical*, 158, 559 – 565.
- Jim C. (2007). Types of Catalysis. Retrieved from <http://www.chemguide.co.uk/catalysis/introduction.html/#top> on 7/8/2010.
- Matsura I., Ruiz P. and Delmon P. (1995). Preparation of precursor: New developments in selective oxidation by heterogeneous catalysis. Elsevier Science Publisher, Amsterdam.

- Meisel M., Wolf G. U. and Bruckner A. (1992). Proceedings DGMK Conference on Selective Oxidations in Petrochemistry. Ed. M. Barnes and J. Weitkamp Tagungsbericht, 9204, 27.
- Nexant's ChemSystems Process Evaluation Research Planning (PERP) (2005). PERP Program-Maleic Anhydride-New Report Alert. Retrieved from <http://www.chemsystems.com/search/docs/abstracts/0304-7-abs.pdf> on 11/9/2010.
- Ramasamy A. V. (2002). Catalysis and theoretical concepts: Catalysis principles and applications. 3<sup>rd</sup> Edition, Narosa Publishing House.
- Richter F., Papp H., Wolf G. U., Gotze T. and Kubias H. (1999). Study of the surface composition of vanadyl pyrophosphate catalysts by XPS and ISS – influence of  $\text{Cs}^{2+}$  and water vapour on the surface P/V ratio of  $(\text{VO})_2\text{P}_2\text{O}_7$ . Analytical Chemistry, 365, 150 – 153.
- Robert W. W. and Glenn L. S. (1986). Vanadium-phosphorus-oxygen industrial catalysts for *n*-butane oxidation: Characterization and kinetic measurements. Ind. 25, 612 – 620.
- ScienceStuff (2002). The production of maleic anhydride. Retrieved from <http://www.vanadium.com.au/ScienceStuff/Chemistry/MaleicAnhydride.htm> on 3/10/2010
- Shina K. and Hatano M. (1997). Maleic anhydride by heterogeneous oxidation of *n*-butane. Applied Surface Science, 121/122, 452 – 460.
- Somorjai G. A. (1994). Introduction to Surface Chemistry and Catalysis. Wiley, New York.
- Taufiq-Yap Y. H., Leong L. K., Hussein M. Z. and Abdul Hamid S. B. (2004). Synthesis and characterisation of vanadyl pyrophosphate catalysts via vanadyl hydrogen phosphate sesquihydrate precursor. Catalysis Today 93 – 95, 715 – 722.
- Taufiq-Yap Y. H., Looi M. H., Hussein M. Z. and Zainal Z. (2002). Investigation of Vanadyl Pyrophosphate Catalysts synthesised from Three Different Routes. Vol 14, Nos 3 – 4, 1494 – 1502.
- Taufiq-Yap Y. H., Looi M. H., Wong Y. N. and Hussein M. Z. (2001). Physicochemical Characterization of Vanadium Phosphorus Catalysts Prepared in Organic and Aqueous Medium. Jurnal Teknologi (34C), 17 – 24.
- Taufiq-Yap Y. H. and Saw C. S. (2007). Effect of different calcinations environments on the vanadium phosphate for selective oxidation of propane and *n*-butane. Catalysis Today 131, 285 – 291.

Zazhigalov V. A., Haber J., Stoch J., Pyanitzkaya A., Komashko G. A. and V. M. (1993). Properties of cobalt promoted  $(VO)_2P_2O_7$  in the oxidation of butane. *Applied Catalysis: A General*, 96, 135 – 150.

## APPENDICES

### APPENDIX A: Volume of Isobutanol Used

Molecular formula of vanadyl phosphate dihydrate =  $\text{VOPO}_4 \cdot 2\text{H}_2\text{O}$

Molecular weight of Vanadium = 50.9414 g/mol

Molecular weight of Phosphate = 30.97376 g/mol

Molecular weight of Oxygen = 15.9994 g/mol

Molecular weight of Hydrogen = 1.0079 g/mol

Molecular weight of  $\text{VOPO}_4 \cdot 2\text{H}_2\text{O}$  = 50.9414 g/mol +  $(7 \times 15.9994 \text{ g/mol})$  +  
 $30.97376 \text{ g/mol} + (4 \times 1.0079 \text{ g/mol})$   
 = 197.94256 g/mol

No. of mol of  $\text{VOPO}_4 \cdot 2\text{H}_2\text{O}$  =  $\frac{\text{mass}}{\text{molecular weight}}$

=  $\frac{10 \text{ g}}{197.94256 \text{ g/mol}}$

= 0.05052 mol

(50 mol alcohol/ mol  $\text{VOPO}_4 \cdot 2\text{H}_2\text{O}$ )

For 1 mol of  $\text{VOPO}_4 \cdot 2\text{H}_2\text{O}$ , 50 mol of alcohol (iso-butanol) is needed.

From the calculation as shown above, 0.05052 mol of  $\text{VOPO}_4 \cdot 2\text{H}_2\text{O}$  is used.

$$\frac{0.05052 \text{ mol VOPO}_4 \cdot 2\text{H}_2\text{O}}{1 \text{ mol VOPO}_4 \cdot 2\text{H}_2\text{O}} \times 50 \text{ mol alcohol} = 2.5260 \text{ mol alcohol}$$

Thus, 2.5260 mol of alcohol (iso-butanol) is needed for 0.05052 mol of VOPO<sub>4</sub> · 2H<sub>2</sub>O.

$$\text{Molecular formula of iso-butanol} = \text{C}_4\text{H}_{10}\text{O}$$

$$\text{Molecular weight of Carbon} = 12.011 \text{ g/mol}$$

$$\text{Molecular weight of Oxygen} = 15.9994 \text{ g/mol}$$

$$\text{Molecular weight of Hydrogen} = 1.0079 \text{ g/mol}$$

$$\text{Molecular weight of C}_4\text{H}_{10}\text{O} = (4 \times 12.011 \text{ g/mol}) + (10 \times 1.0079 \text{ g/mol})$$

$$+ 15.9994 \text{ g/mol}$$

$$= 74.1224 \text{ g/mol}$$

$$\text{Density of C}_4\text{H}_{10}\text{O} = 0.802 \text{ g/cm}^3 \text{ at } 20 \text{ }^\circ\text{C}$$

$$\text{Mass of C}_4\text{H}_{10}\text{O} = 74.1224 \text{ g/mol} \times 2.5260 \text{ mol}$$

$$= 187.2332 \text{ g}$$

$$\text{Density} = \frac{\text{mass}}{\text{volume}}$$

$$\text{Volume of iso-butanol} = \frac{\text{mass}}{\text{density}}$$

$$= \frac{187.2332 \text{ g}}{0.802 \text{ g/cm}^3}$$

$$= 233.4578 \text{ cm}^3$$

Therefore, total volume of iso-butanol added is 233.4578 cm<sup>3</sup>.

**APPENDIX B: Volume of Distilled Water Used**

(24 ml H<sub>2</sub>O/ g solid)

15 g of V<sub>2</sub>O<sub>5</sub> is used as a starting material.

Thus, the volume of distilled water needed = 15 g × (24 ml H<sub>2</sub>O/ g solid)  
= 360 ml

**APPENDIX C: Crystallite Size Measurement (XRD Analysis)**

Crystallite size, T given by Debye-Scherrer equation:  $T(\text{\AA}) = \frac{0.89\lambda}{FWHM \times \cos\theta}$

Given  $\lambda_{\text{Cu K}\alpha} = 1.54\text{\AA}$

$$FWHM (\text{rad}) = FWHM (^\circ) \times \frac{\pi}{180^\circ}$$

**APPENDIX D: Preparation of Diphenylamine, Ph<sub>2</sub>NH Indicator  
(Redox Titration)**

1 g of diphenylamine was weighed and dissolved in a few ml of concentrated sulphuric acid, H<sub>2</sub>SO<sub>4</sub>. Then the solution was transferred to a 100 ml volumetric flask and further top up with concentrated H<sub>2</sub>SO<sub>4</sub>.

### APPENDIX E: Preparation of 2 M Sulphuric Acid, H<sub>2</sub>SO<sub>4</sub> Solution

Concentrated H<sub>2</sub>SO<sub>4</sub> (95- 98%)

$$1\text{L} = 1.84 \text{ kg} = 1840 \text{ g} / 1000\text{cm}^3 = 1.84 \text{ g/cm}^3$$

$$\begin{aligned} \text{Molecular weight of H}_2\text{SO}_4 &= 2(1.00 \text{ g/mol}) + 32.07 \text{ g/mol} + 4(16.00 \text{ g/mol}) \\ &= 98.07 \text{ g/mol} \end{aligned}$$

$$\text{Concentration of 95- 98\% H}_2\text{SO}_4 = \frac{1.84 \text{ g/cm}^3}{98.07 \text{ g/mol}} \times \frac{95}{100} \times 1000 = 17.82 \text{ M}$$

$$M_1 V_1 = M_2 V_2 \quad \text{where } M_1 = \text{concentration of 95- 98\% H}_2\text{SO}_4$$

$$M_2 = \text{concentration of diluted H}_2\text{SO}_4 (2 \text{ M})$$

$$V_1 = \text{volume of 95- 98\% H}_2\text{SO}_4$$

$$V_2 = \text{volume of diluted H}_2\text{SO}_4 (2 \text{ M})$$

$$(17.82 \text{ M}) (V_1) = (2 \text{ M}) (1000 \text{ cm}^3)$$

$$V_1 = 112.23 \text{ cm}^3$$

**APPENDIX F: Preparation of 0.1 M Sulphuric Acid, H<sub>2</sub>SO<sub>4</sub> Solution**

$$M_1 V_1 = M_2 V_2$$

where  $M_1$  = concentration of 95- 98% H<sub>2</sub>SO<sub>4</sub>

$M_2$  = concentration of diluted H<sub>2</sub>SO<sub>4</sub> (0.1 M)

$V_1$  = volume of 95- 98% H<sub>2</sub>SO<sub>4</sub>

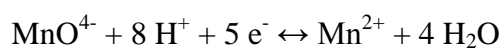
$V_2$  = volume of diluted H<sub>2</sub>SO<sub>4</sub> (0.1 M)

$$(17.82 \text{ M}) (V_1) = (0.1 \text{ M}) (1000 \text{ cm}^3)$$

$$V_1 = 5.61 \text{ cm}^3$$

**APPENDIX G: Preparation of 0.01 N Potassium Permanganate,  $\text{KMnO}_4$**   
**(Redox Titration)**

$$\text{Normality, } N \text{ (eq/L)} = M \text{ (mol/L)} \times n \text{ (eq/mol)}$$



$$\text{Molarity, } M \text{ (mol/L)} = \frac{N \text{ (eq/L)}}{n \text{ (eq/mol)}}$$

$$= \frac{0.01}{5}$$

$$= 0.002 \text{ M}$$

$$\text{Molecular weight for } \text{KMnO}_4 = 39.10 \text{ g/mol} + 54.94 \text{ g/mol} + 4 (16.00 \text{ g/mol})$$

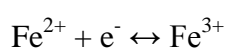
$$= 158.04 \text{ g/mol}$$

$$\text{Weight for } \text{KMnO}_4 \text{ in } 1000 \text{ cm}^3 \text{ diluted (0.1 M) } \text{H}_2\text{SO}_4 = 0.002 \times 158.04$$

$$= 0.3161 \text{ g}$$

**APPENDIX H: Preparation of 0.01 N ammonium iron(II) sulphate,  
(NH<sub>4</sub>)<sub>2</sub>Fe(SO<sub>4</sub>)<sub>2</sub> 6H<sub>2</sub>O (Redox Titration)**

$$\text{Normality, N (eq/L)} = \text{M (mol/L)} \times n \text{ (eq/mol)}$$



$$\begin{aligned} \text{Molarity, M (mol/L)} &= \frac{N(\text{eq/L})}{n(\text{eq/mol})} \\ &= \frac{0.01}{1} \\ &= 0.01 \text{ M} \end{aligned}$$

$$\begin{aligned} \text{Molecular weight for (NH}_4\text{)}_2\text{Fe(SO}_4\text{)}_2 \cdot 6\text{H}_2\text{O} &= 2 (14.00 \text{ g/mol}) + 20 (1.00 \text{ g/mol}) \\ &\quad + 55.85 \text{ g/mol} + 2 (32.07 \text{ g/mol}) + \\ &\quad 14 (16.00 \text{ g/mol}) \\ &= 391.99 \text{ g/mol} \end{aligned}$$

$$\begin{aligned} \text{Weight for (NH}_4\text{)}_2\text{Fe(SO}_4\text{)}_2 \cdot 6\text{H}_2\text{O in } 1000 \text{ cm}^3 \text{ diluted (0.1 M) H}_2\text{SO}_4 \\ &= 0.01 \times 392.14 \\ &= 3.9214 \text{ g} \end{aligned}$$

### APPENDIX I: Oxidation State of Vanadium (Redox Titration)

According to Niwa and Murakami (1982),

$$T_1 = V^{4+} + 2V^{3+} = 20 [\text{MnO}_4^-] V_1 \quad (1)$$

$$T_2 = V^{5+} + V^{4+} + V^{3+} = 20 [\text{Fe}^{2+}] V_2 \quad (2)$$

$$T_3 = V^{5+} = 20 [\text{Fe}^{2+}] V_3 \quad (3)$$

$$(2) - (3): \quad V^{3+} + V^{4+} = 20 [\text{Fe}^{2+}] V_2 - 20 [\text{Fe}^{2+}] V_3 \quad (4)$$

$$(1) - (4): \quad V^{3+} = 20 [\text{MnO}_4^-] V_1 - 20 [\text{Fe}^{2+}] V_2 + 20 [\text{Fe}^{2+}] V_3 \quad (5)$$

Substitute (5) into (1):

$$V^{4+} + 2(20 [\text{MnO}_4^-] V_1 - 20 [\text{Fe}^{2+}] V_2 + 20 [\text{Fe}^{2+}] V_3) = 20 [\text{MnO}_4^-] V_1$$

$$\begin{aligned} V^{4+} &= 20 [\text{MnO}_4^-] V_1 - 40 [\text{MnO}_4^-] V_1 + 40 [\text{Fe}^{2+}] V_2 - 40 [\text{Fe}^{2+}] V_3 \\ &= 40 [\text{Fe}^{2+}] V_2 - 40 [\text{Fe}^{2+}] V_3 - 20 [\text{MnO}_4^-] V_1 \end{aligned} \quad (6)$$

Substitute (5) and (6) into (2):

$$\begin{aligned} 20 [\text{Fe}^{2+}] V_2 &= V^{5+} + (40 [\text{Fe}^{2+}] V_2 - 40 [\text{Fe}^{2+}] V_3 - 20 [\text{MnO}_4^-] V_1) + (20 [\text{MnO}_4^-] V_1 \\ &\quad - 20 [\text{Fe}^{2+}] V_2 + 20 [\text{Fe}^{2+}] V_3) \end{aligned}$$

$$V^{5+} = 20 [\text{Fe}^{2+}] V_3 \quad (7)$$

$$\begin{aligned} \text{From (5):} \quad V^{3+} &= 20 (0.01) V_1 - 20 (0.01) V_2 + 20 (0.01) V_3 \\ &= 0.2 (V_1 - V_2 + V_3) \end{aligned} \quad (8)$$

$$\begin{aligned}
 \text{From (6): } V^{4+} &= 40 (0.01) V_2 - 40 (0.01) V_3 - 20 (0.01) V_1 \\
 &= 0.4 V_2 - 0.4 V_3 - 0.2 V_1
 \end{aligned} \tag{9}$$

$$\begin{aligned}
 \text{From (7): } V^{5+} &= 20 (0.01) V_3 \\
 &= 0.2 V_3
 \end{aligned} \tag{10}$$

The average vanadium valence is calculated as:

$$V_{AV} = \frac{3V^{3+} + 4V^{4+} + 5V^{5+}}{V^{3+} + V^{4+} + V^{5+}} \tag{11}$$

#### VPSA24

$$V_1 = 10.75, V_2 = 12.0, V_3 = 2.13$$

$$\begin{aligned}
 \text{From (6): } V^{4+} &= 40 (0.01) V_2 - 40 (0.01) V_3 - 20 (0.01) V_1 \\
 &= 0.4 V_2 - 0.4 V_3 - 0.2 V_1 \\
 &= 0.4 (12.0) - 0.4 (2.13) - 0.2 (10.75) \\
 &= 1.798
 \end{aligned}$$

$$\begin{aligned}
 \text{From (7): } V^{5+} &= 20 (0.01) V_3 \\
 &= 0.2 V_3 \\
 &= 0.2 (2.13) \\
 &= 0.426
 \end{aligned}$$

The average vanadium valence is calculated as:

$$V_{AV} = \frac{3V^{3+} + 4V^{4+} + 5V^{5+}}{V^{3+} + V^{4+} + V^{5+}}$$

$$= \frac{3(0) + 4(1.798) + 5(0.426)}{0 + 1.798 + 0.426}$$

$$= 4.1915$$

If  $V_{AV}$  of sample A = 4.1915

$$V^{5+} (\%) = 19.15 \%$$

$$V^{4+} (\%) = (100 - 19.15) \%$$

$$= 80.85 \%$$

#### VPO24

$$V_1 = 11.6, V_2 = 12.1, V_3 = 1.63$$

$$\begin{aligned} \text{From (6): } V^{4+} &= 40 (0.01) V_2 - 40 (0.01) V_3 - 20 (0.01) V_1 \\ &= 0.4 V_2 - 0.4 V_3 - 0.2 V_1 \\ &= 0.4 (12.1) - 0.4 (1.63) - 0.2 (11.6) \\ &= 1.868 \end{aligned}$$

$$\begin{aligned} \text{From (7): } V^{5+} &= 20 (0.01) V_3 \\ &= 0.2 V_3 \\ &= 0.2 (1.63) \\ &= 0.326 \end{aligned}$$

The average vanadium valence is calculated as:

$$V_{AV} = \frac{3V^{3+} + 4V^{4+} + 5V^{5+}}{V^{3+} + V^{4+} + V^{5+}}$$

$$= \frac{3(0) + 4(1.868) + 5(0.326)}{0 + 1.868 + 0.326}$$

$$= 4.1486$$

If  $V_{AV}$  of sample B = 4.1486

$$V^{5+} (\%) = 14.86 \%$$

$$V^{4+} (\%) = (100 - 14.86) \%$$

$$= 85.14 \%$$

## VPD24

$$V_1 = 9.7, V_2 = 10.75, V_3 = 1.93$$

$$\begin{aligned} \text{From (6): } V^{4+} &= 40 (0.01) V_2 - 40 (0.01) V_3 - 20 (0.01) V_1 \\ &= 0.4 V_2 - 0.4 V_3 - 0.2 V_1 \\ &= 0.4 (10.75) - 0.4 (1.93) - 0.2 (9.7) \\ &= 1.588 \end{aligned}$$

$$\begin{aligned} \text{From (7): } V^{5+} &= 20 (0.01) V_3 \\ &= 0.2 V_3 \\ &= 0.2 (1.93) \\ &= 0.386 \end{aligned}$$

The average vanadium valence is calculated as:

$$V_{AV} = \frac{3V^{3+} + 4V^{4+} + 5V^{5+}}{V^{3+} + V^{4+} + V^{5+}}$$

$$= \frac{3(0) + 4(1.588) + 5(0.386)}{0 + 1.588 + 0.386}$$

$$= 4.1955$$

If  $V_{AV}$  of sample C = 4.1955

$$V^{5+} (\%) = 19.55 \%$$

$$V^{4+} (\%) = (100 - 19.55) \%$$

$$= 80.45 \%$$

#### VPS24

$$V_1 = 10.8, V_2 = 12.0, V_3 = 2.13$$

$$\begin{aligned} \text{From (6): } V^{4+} &= 40 (0.01) V_2 - 40 (0.01) V_3 - 20 (0.01) V_1 \\ &= 0.4 V_2 - 0.4 V_3 - 0.2 V_1 \\ &= 0.4 (12.0) - 0.4 (2.13) - 0.2 (10.8) \\ &= 1.788 \end{aligned}$$

$$\begin{aligned} \text{From (7): } V^{5+} &= 20 (0.01) V_3 \\ &= 0.2 V_3 \\ &= 0.2 (2.13) \\ &= 0.426 \end{aligned}$$

The average vanadium valence is calculated as:

$$\begin{aligned}V_{AV} &= \frac{3V^{3+} + 4V^{4+} + 5V^{5+}}{V^{3+} + V^{4+} + V^{5+}} \\&= \frac{3(0) + 4(1.788) + 5(0.426)}{0 + 1.788 + 0.426} \\&= 4.1924\end{aligned}$$

If  $V_{AV}$  of sample C = 4.1924

$$V^{5+} (\%) = 19.24 \%$$

$$\begin{aligned}V^{4+} (\%) &= (100 - 11.26) \% \\&= 88.74 \%\end{aligned}$$